DNA Damage and Repair

Molecular Cancer Research

Angiopoietin-like Protein 2 Accelerates Carcinogenesis by Activating Chronic Inflammation and Oxidative Stress

Jun Aoi[1,2], Motoyoshi Endo[1], Tsuyoshi Kadomatsu[1], Keishi Miyata[1], Aki Ogata[1,2], Haruki Horiguchi[1], Haruki Odagiri[1], Tetsuro Masuda[1], Satoshi Fukushima[2], Masatoshi Jinnin[2], Satoshi Hirakawa[3], Tomohiro Sawa[4,5], Takaaki Akaike[4], Hironobu Ihn[2], and Yuichi Oike[1,6]

Abstract

Chronic inflammation has received much attention as a risk factor for carcinogenesis. We recently reported that Angiopoietin-like protein 2 (Angptl2) facilitates inflammatory carcinogenesis and metastasis in a chemically induced squamous cell carcinoma (SCC) of the skin mouse model. In particular, we demonstrated that Angptl2-induced inflammation enhanced susceptibility of skin tissues to "preneoplastic change" and "malignant conversion" in SCC development; however, mechanisms underlying this activity remain unclear. Using this model, we now report that transgenic mice overexpressing Angptl2 in skin epithelial cells (K14-*Angptl2* Tg mice) show enhanced oxidative stress in these tissues. Conversely, in the context of this model, *Angptl2* knockout (KO) mice show significantly decreased oxidative stress in skin tissue as well as a lower incidence of SCC compared with wild-type mice. In the chemically induced SCC model, treatment of K14-*Angptl2* Tg mice with the antioxidant *N*-acetyl cysteine (NAC) significantly reduced oxidative stress in skin tissue and the frequency of SCC development. Interestingly, K14-*Angptl2* Tg mice in the model also showed significantly decreased expression of mRNA encoding the DNA mismatch repair enzyme Msh2 compared with wild-type mice and increased methylation of the *Msh2* promoter in skin tissues. *Msh2* expression in skin tissues of Tg mice was significantly increased by NAC treatment, as was *Msh2* promoter demethylation. Overall, this study strongly suggests that the inflammatory mediator Angptl2 accelerates chemically induced carcinogenesis through increased oxidative stress and decreased *Msh2* expression in skin tissue.

Implications: Angptl2-induced inflammation increases susceptibility to microenvironmental changes, allowing increased oxidative stress and decreased Msh2 expression; therefore, Angptl2 might be a target to develop new strategies to antagonize these activities in premalignant tissue. *Mol Cancer Res; 12(2); 239–49. ©2013 AACR.*

Introduction

The connection between cancer and inflammation was first made in the 19th century (1). Since then, epidemiologic studies have confirmed the idea that chronic inflammation underlies many cancers (2). Recently, we reported that Angiopoietin-like protein 2 (Angptl2) acts as a chronic inflammatory mediator in several pathologic settings (3–6), and demonstrated that increased Angptl2 expression in skin tissues promotes inflammation and accelerates carcinogenesis in a chemically induced squamous cell carcinoma (SCC) of the skin mouse model by increasing susceptibility to "preneoplastic change" and "malignant conversion" (7). In normal cells, initiating oncogenic mutation is considered essential to promote a "preneoplastic change," which, if unrepaired, is then followed by proliferation and acquisition of cellular survival capacity, allowing accumulation of additional mutations (8–10). Potentially oncogenic mutations can be antagonized by DNA repair mechanisms, some mediated by members of the mismatch repair (MMR) family, which corrects base mispairings or repairs larger insertion/deletion loops (IDL; refs 11–14). In the MMR system, three homologs of the bacterial MutS protein—Msh2, Msh3, and Msh6—form heterodimers that recognize DNA damage (15). Loss-of-function mutations or epigenetic silencing of MMR genes increase genomic microsatellite instability (MSI), increasing the rate of DNA replication errors (16). Genetic and biochemical studies indicate that Msh2 is a critical component of all MMR complexes and, consequently, *Msh2*-null mutants are predicted to completely the lack

Authors' Affiliations: Departments of [1]Molecular Genetics and [2]Dermatology and Plastic Surgery, Graduate School of Medical Sciences, Kumamoto University, Kumamoto; [3]Department of Dermatology, Hamamatsu University School of Medicine, Hamamatsu; [4]Department of Environmental Health Sciences and Molecular Toxicology, Tohoku University Graduate School of Medicine, Sendai; [5]PRESTO, Japan Science and Technology Agency, Kawaguchi, Saitama, Japan; and [6]Core Research for Evolutional Science and Technology (CREST), Japan Science and Technology Agency, Tokyo, Japan

Note: Supplementary data for this article are available at Molecular Cancer Research Online (http://mcr.aacrjournals.org/).

Corresponding Authors: Yuichi Oike, Department of Molecular Genetics, Graduate School of Medical Sciences, Kumamoto University, 1-1-1 Honjo, Kumamoto 860-8556, Japan. Phone: 81-96-373-5142; Fax: 81-96-373-5145; E-mail: oike@gpo.kumamoto-u.ac.jp; and Motoyoshi Endo, E-mail: enmoto@gpo.kumamoto-u.ac.jp

doi: 10.1158/1541-7786.MCR-13-0336

MMR response (17, 18). Significantly, loss or mutation of mammalian *Msh2* increases the probability of developing certain types of tumors (19).

In this study, we report that K14-*Angptl2* Tg mice, which show accelerated skin tissue inflammation and greater frequency of chemically induced SCC, showed enhanced oxidative stress in skin tissues and decreased expression of *Msh2*, likely due to increased methylation of the *Msh2* promoter. Interestingly, treatment of these mice with the antioxidant *N*-acetyl cysteine (NAC) significantly reduced oxidative stress in skin tissue and SCC frequency. Furthermore, *Msh2* mRNA expression in skin tissue of Tg mice significantly increased following NAC treatment in parallel with demethylation of the *Msh2* promoter region. Overall, these findings suggest that Angptl2-induced inflammation increases susceptibility to microenvironmental changes allowing accumulation of oncogenic DNA mutations.

Materials and Methods

Mice

Male mice were used for the experiments. Mice were housed in a temperature-controlled room with a 12-hour light/dark cycle. Food and water were available *ad libitum* unless otherwise noted. Mice were fed a normal diet (CE-2; CLEA, Japan). For some experiments, NAC (40 mmol/L) was administered in drinking water from 7 weeks after birth until the end of the experiments. For chemical carcinogenesis assays, K14-*Angptl2* Tg (3) and *Angptl2* KO (3) were backcrossed to the FVB/N strain for more than 10 generations. During the course of the experiment, we observed no significant difference in body weight between K14-*Angptl2* Tg and wild-type littermate mice or between *Angptl2* KO and wild-type littermates. In addition, we observed no significant difference in body weight between these groups, with or without NAC treatment. All experiments were performed according to the guidelines of the Institutional Animal Committee of Kumamoto University.

Chemically induced skin carcinogenesis

We performed chemical skin carcinogenesis experiments using K14-*Angptl2* Tg mice, *Angptl2* KO mice, and respective wild-type littermates as controls, as described previously (20, 21). Briefly, 50 μg of the chemical initiator mutagen 7,12-dimethylbenzanthracene (DMBA; Sigma) was applied topically to the shaved skin on the back of 8-week-old male mice, followed by weekly topical application of 5 μg of the tumor promoter phorbol ester 12-O-tetradecanoylphorbol 13-acetate (PMA; Sigma) over 20 weeks. Raised lesions of a minimum diameter of 1 mm present for at least 1 week were scored as papillomas. Large papillomas were defined as papillomas of 3 mm or more in diameter. Mice were killed after 45 weeks or at 8 weeks after the first diagnosis of SCC. SCC evaluation was carried out clinically and histologically by two independent dermatologists using specified standards (20–22). Clinically, SCCs are significantly larger and grow more rapidly than papillomas. Histologically, papillomas show loss of polarity and anaplasia of the nuclei localized to the epidermis. However, SCCs are invasive carcinomas of the surface epidermis. SCCs proliferate downward into the dermis. The ratio of malignant conversion was calculated for each group of mice as the total number of SCC divided by the number of large papillomas and expressed as a percentage. The two-sided unpaired Student *t*-test was used to analyze differences in the number of tumors per mice with or without NAC treatment.

Immunoblot analysis

Skin tissues were homogenized in lysis buffer (10 mmol/L NaF, 1 mmol/L Na_3VO_4, 1 mmol/L EDTA, 300 mmol/L NaCl, 50 mmol/L Tris–HCl, pH 7.5, and 1% Triton X-100). Extracts derived from supernatants were subjected to SDS–PAGE electrophoresis, and proteins were electrotransferred to nitrocellulose membranes. Immunodetection was performed using an ECL kit (Amersham) according to the manufacturer's instructions. Antibodies against 4-hydroxy-2-nonenal (4-HNE; Santa Cruz Biotechnology), Hsc70 (B-6; R&D Systems), Rad51, Brca2, Atm, Atr, Ku70, Ku80, and Msh2 (Cell Signaling Technology), and Angptl2 (3) were used.

Immunohistochemical staining

Skin tissues were fixed by perfusion with 4% paraformaldehyde in PBS (pH 7.4), washed in PBS for 15 minutes, dehydrated through a graded series of ethanols and xylene, and embedded in a single paraffin block. Sections (5 μm) were cut, air-dried, deparaffinized, and pretreated with 5 mmol/L periodic acid for 10 minutes at room temperature to inhibit endogenous peroxidase. Specimens were incubated for 1 hour with 50- to 100-fold diluted polyclonal antibody against Angptl2 (3) or Msh2 (Cell Signaling Technology), and then washed 3 times with PBS for 5 minutes. Sections were incubated with biotinylated anti-mouse IgG or anti-rabbit IgG (1:200 dilution; Vector Laboratories). Immunostaining was performed using the peroxidase-labeled avidin–biotin–complex method (1:100 dilution; DAKO). Sections were counterstained with hematoxylin.

DNA extraction and bisulfate modification

DNA was isolated from skin tissues using the SDS/proteinase K method. DNA concentration was determined spectrophotometrically at 260 nm. DNA bisulfite treatment was used to convert unmethylated CpG sites to UpG without modifying methylated sites, thus allowing them to be distinguished by restriction digestion using the Combined Bisulfite Restriction Analysis (COBRA) assay (17). Bisulfite treatment of genomic DNA was performed using the MethylEasy *Xceed* Rapid DNA Bisulphite Modification Kit (Human Genetic Signatures) according to the manufacturer's instructions. CpG-methylated NIH 3T3 mouse genomic DNA (New England Biolabs) served as a positive control and underwent bisulfite modification as described earlier. NIH 3T3 mouse genomic DNA (New England Biolabs) served as a negative control. The proportion of methylated versus unmethylated product (digested vs. undigested) was quantified by densitometry (23). Densitometric analysis was performed using Multi Gauge software (Fujifilm).

PCR and restriction digestion

Msh2 primers were specially designed for the COBRA assay as described previously (17). Sequences used were 5′-TGGCGGTGTAGTTTAAGGAGA-3′ (forward) and 5′-TCTTAAACACCTCGCGAACC-3′ (reverse), generating a 195-bp amplification product (17). PCR amplifications were performed using TaKaRa EpiTaq HS (for bisulfite-treated DNA; Takara Bio) according to the manufacturer's instructions. After amplification, PCR products were digested with *Mbo*I (Promega), which cuts DNA harboring a d (GATC) target site only if the site is retained after bisulfite-mediated deamination. Samples were separated on 2% agarose gels, which were then stained with ethidium bromide. The proportion of methylated versus unmethylated product (digested vs. undigested) was quantified by densitometry (17, 23) using MultiGauge version 3.1 software (Fuji Film).

Calculation of survival data

A Kaplan–Meier log-rank test was applied to analyze mouse survival data using JMP7 software (SAS Institute). A P value of less than 0.05 was considered significant.

Real-time quantitative RT-PCR

For mouse skin tissues, total RNA was isolated using the TRIzol reagent (Invitrogen). DNase-treated RNA was reverse transcribed with a PrimeScript RT reagent Kit (Takara Bio). PCR products were analyzed with a Thermal Cycler Dice Real Time system (Takara Bio), and relative transcript abundance was normalized to that of *18S* mRNA. PCR oligonucleotides were as follows: mouse *Msh2*: forward, 5′-GCCCAGGATGCCATTGTTAAAG-3′, reverse, 5′-AACGGGTGCTGCGTTTGAC-3′: mouse *18S*: forward, 5′-TTCTGGCCAACGGTCTAGACAAC-3′, reverse, 5′-CCAGTGGTCTTGGTGTGCTGA-3′: mouse *IL-1β*: forward, 5′- TCCAGGATGAGGACATGAGCAC-3′, reverse, 5′- GAACGTCACACACCAGCAGGTTA-3′: mouse *IL-6*: forward, 5′- CCACTTCACAAGTCGGAGGCTTA-3′, reverse, 5′- GCAAGTGCATCATCGTTGTTCATAC-3′. Results were analyzed using the two-tailed Student t-test with Excel software (Microsoft). A P value of less than 0.05 was considered significant.

Clinical characterization of patients

For ANGPTL2 and MSH2 immunostaining, we obtained normal abdominal skin tissues, as well as tissues derived by curative resection from patients with actinic keratosis and squamous cell carcinoma on the face (at Kumamoto University). Diagnostic evaluation of human samples was carried out by two independent dermatologists clinically and histologically. All studies were approved by the Ethics Committee of Kumamoto University. Written informed consent was obtained from each subject.

Results

Increased oxidative stress parallels Angptl2 expression in mouse skin tissues

Initially, we confirmed our previous findings regarding differences in susceptibility to chemically induced carcinogenesis among K14-*Angptl2* Tg, wild-type, and *Angptl2* KO mice by estimating the frequency and time course of SCC development in mice of all three genotypes. As we previously reported, increased Angptl2 expression in skin tissues accelerated carcinogenesis in the SCC model (Fig. 1A), whereas Angptl2 loss antagonized carcinogenesis (Fig. 1B). Seven weeks after initiation of chemical treatment, K14-*Angptl2* Tg, *Angptl2* KO, and respective wild-type mice showed little evidence of papillomas or SCC in chemically treated skin

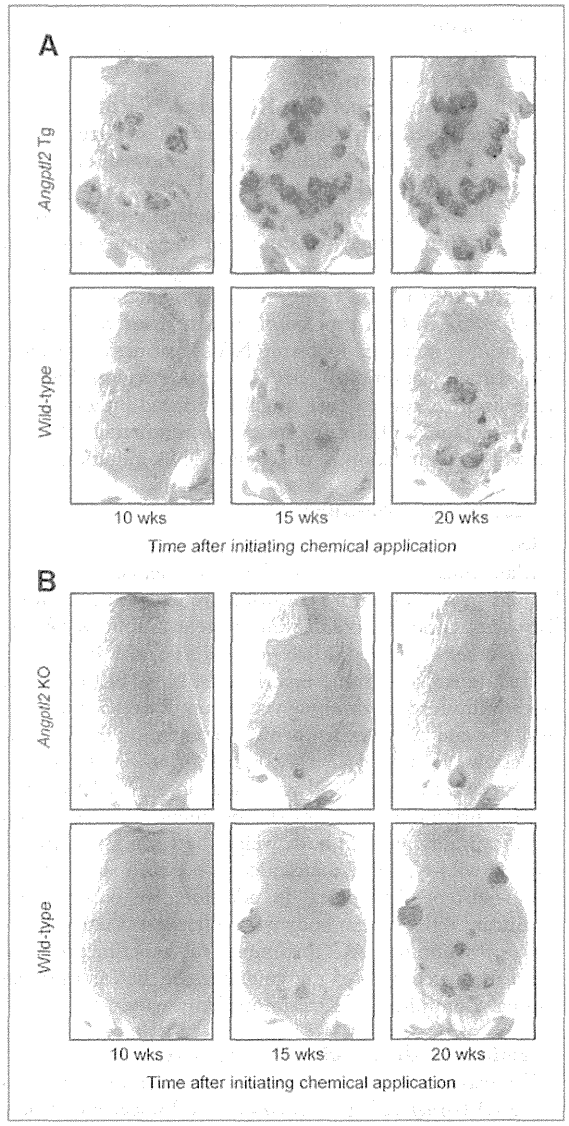

Figure 1. Chemical skin carcinogenesis is accelerated in skin tissues constitutively expressing Angptl2 and suppressed in *Angptl2*-deficient tissues. A and B, representative photographs showing the same mouse (in each row) throughout the time course of chemical skin carcinogenesis from both K14-*Angptl2* Tg and wild-type littermates (A) and *Angptl2* KO and wild-type littermates (B) at 10 (left), 15 (middle), and 20 (right) weeks after initiation of chemical application.

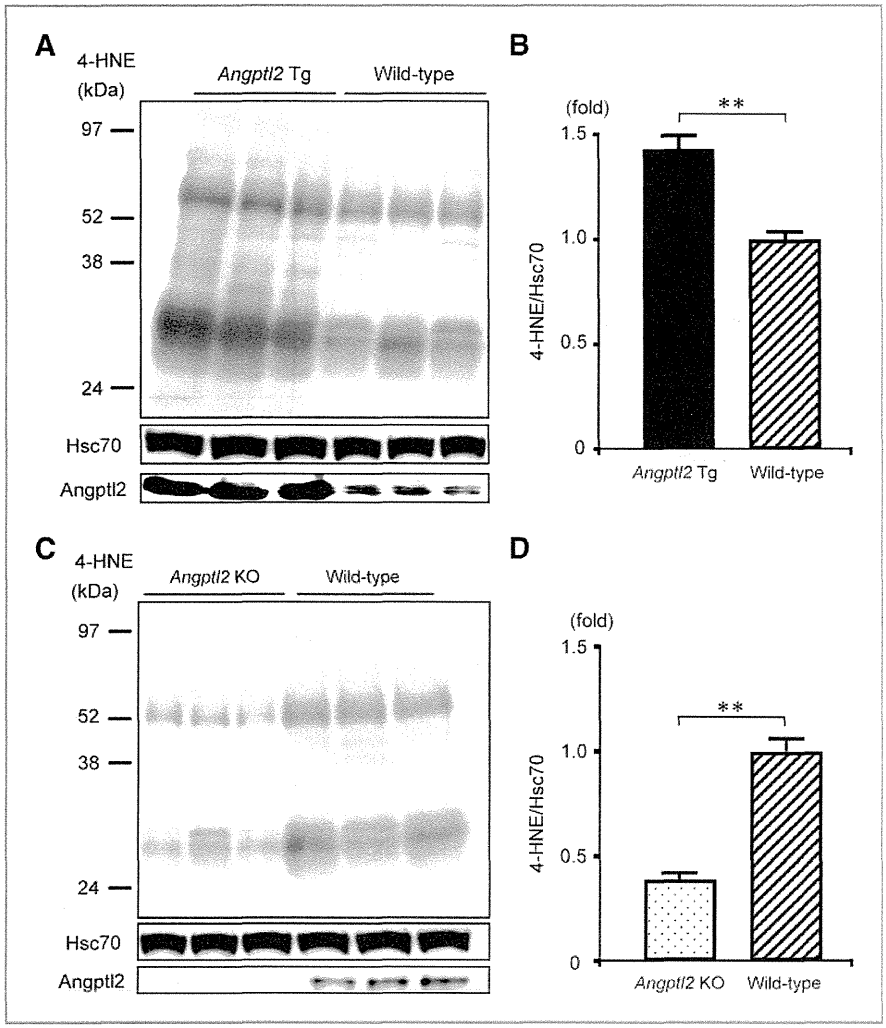

Figure 2. ROS levels increase in skin tissues of K14-*Angptl2* transgenic mice and decrease in tissues from *Angptl2* KO mice. A and C, Western blot analysis using 4-hydroxy-2-nonenal (4-HNE) antibody, which recognizes ROS-modified proteins, of skin tissues of K14-*Angptl2* Tg and wild-type mice (A) and *Angptl2* KO and wild-type mice (C). Skin tissues received a single application of DMBA plus 7 applications of PMA. Hsc70 serves as an internal control. B and D, quantitation of Western blot analysis ($n = 3$) in (B) and (D), (wild-type data set at 1). Graphs show data in the 24 to 97 kDa range. Data are expressed as mean ± SEM. **, $P < 0.01$ compared with wild-type mice.

tissues (data not shown). Therefore, for further study we analyzed skin tissues from the mid-dorsal portion of the back of animals at 7 weeks after beginning chemical application.

In animal tissues, 4-hydroxy-2-nonenal (4-HNE) is a lipid peroxidation product whose formation is closely related to oxidative stress (24). Because of its electrophilic nature, 4-HNE reacts with nucleophilic amino acid residues in proteins to form HNE-adducted proteins. For our studies, we used an HNE-antibody that recognizes HNE-adducted histidine moieties in proteins (HNE-modified proteins) to monitor both the occurrence and extent of oxidative stress in skin tissues (Supplementary Fig. S1). Immunoblot analysis of skin tissues at the 7-week time point using the anti-4-HNE antibody indicated that HNE-modified protein level, in tissues from K14-*Angptl2* Tg mice, significantly increased relative to conditions seen in wild-type mice (Fig. 2A and B). Conversely, levels of HNE-modified proteins in skin tissues of *Angptl2* KO mice were significantly decreased compared with wild-type controls (Fig. 2C and D). In addition, we found that HNE-modified protein levels were positively correlated with the Angptl2 levels (Fig. 2A and C). These findings suggest that Angptl2 increases oxidative stress.

Antioxidant treatment reduces *Angptl2*-associated oxidative stress and decreases papilloma and SCC formation in a SCC model

We previously proposed that Angptl2 expression in skin tissues accelerates chemically induced carcinogenesis by increasing susceptibility to "pre-neoplastic change" and "malignant conversion" (7). To determine whether these changes are attributable to increased oxidative stress in those tissues, we treated mice with the potent antioxidant NAC by including it in their drinking water (25). Immunoblot analysis using anti-4-HNE antibody of skin tissues harvested 7 weeks after initiating chemical application indicated that levels of reactive oxygen species (ROS) in NAC-treated K14-*Angptl2* Tg mice were significantly lower than those seen in Tg mice not treated with NAC (Fig. 3A and B). By 14 weeks

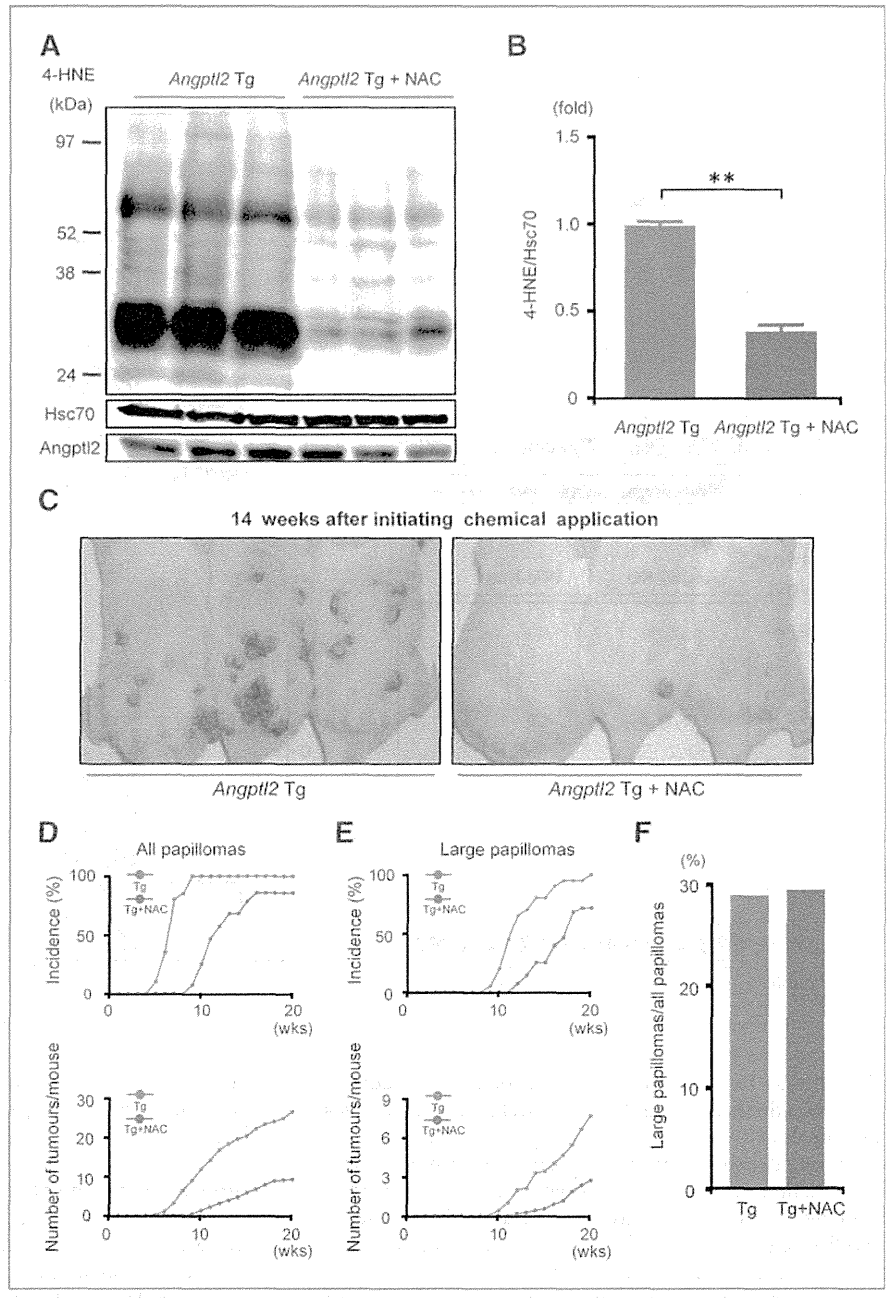

Figure 3. NAC treatment reduces oxidative stress and susceptibility to chemical tumorigenesis in K14-*Angptl2* Tg mice. A and B, Western blot analysis using the 4-hydroxy-2-nonenal (4-HNE) antibody to analyze skin tissues of K14-*Angptl2* Tg mice provided drinking water without (left) or with (right) NAC. Mice were chemically treated as in Fig. 2. Hsc70 serves as an internal control. B, quantitative analysis of Western blot analysis ($n = 3$) of K14-*Angptl2* Tg mice with and without NAC treatment (K14-*Angptl2* Tg without NAC treatment data set at 1). Graphs show data in the 24 to 97 kDa range. Data are expressed as means ± SEM. **, $P < 0.01$ compared with K14-*Angptl2* Tg mice given normal water. C, image showing skin of K14-*Angptl2* Tg mice administered normal (left) and NAC-treated (right) water at 14 weeks after the first chemical application. D and E, top, "incidence" is defined as the percentage of mice with papillomas; bottom, the number of all detectable (1–3 mm) (D) or large (>3 mm) (E) papillomas from K14-*Angptl2* Tg mice provided untreated ($n = 20$; red circles) or NAC-treated ($n = 28$; blue circles) water. $P < 0.005$ from weeks 6 to 20 (in D, bottom), $P < 0.05$ from weeks 10 to 20 (E, bottom). F, proportion of large papillomas seen in K14-*Angptl2* Tg mice provided normal (Tg) or NAC-containing (Tg + NAC) water.

after initiation of chemical treatment, K14-*Angptl2* Tg mice exhibited numerous papillomas in the absence of NAC treatment (Fig. 3C, left), whereas NAC-treated Tg mice showed a significantly reduced number of papillomas (Fig. 3C, right). The average latency is defined as time to reach 50% incidence of all papillomas (7, 26, 27). NAC-treated K14-*Angptl2* mice also showed attenuated formation of skin papillomas, with an average latency of 11 weeks after the beginning of chemical application, as compared with K14-*Angptl2* Tg mice not treated with NAC, which showed an average latency of 7 weeks (Fig. 3D, top). In addition, K14-*Angptl2* Tg mice treated with NAC showed significantly fewer papillomas (Fig. 3D, bottom). After 20 weeks of chemical treatment, NAC-treated K14-*Angptl2* Tg mice exhibited an average of 9.2 papillomas per mouse, whereas K14-*Angptl2* Tg mice without NAC exhibited an average of 26.5 ($P < 1 \times 10^{-9}$). When only large papillomas (diameter > 3 mm) were evaluated, K14-*Angptl2* Tg with treated with

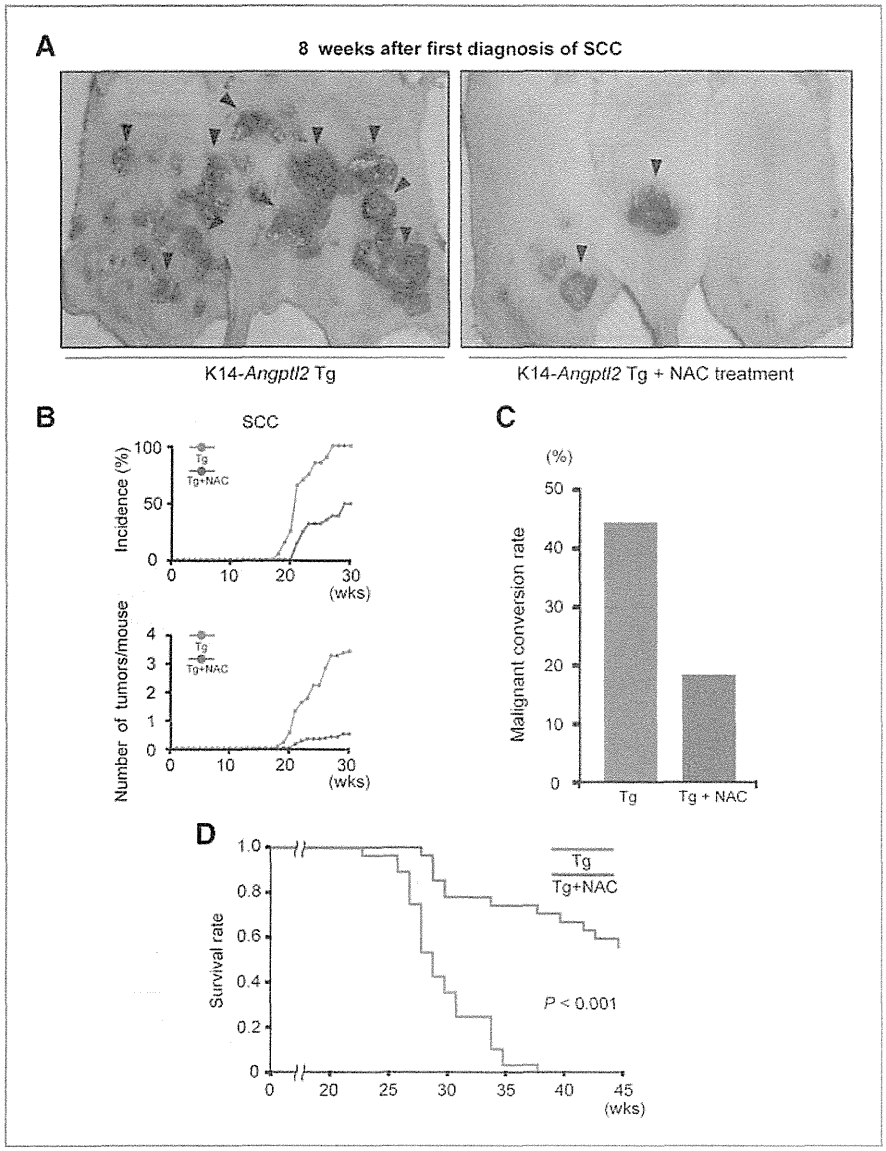

Figure 4. Antioxidant treatment prevents carcinogenesis and prolongs survival of K14-*Angptl2* Tg mice. A, photograph of SCC exhibited by K14-*Angptl2* Tg mice provided normal (left) or NAC-treated (right) water at 8 weeks after first diagnosis of SCC. Arrowheads indicate SCC. B, increased incidence of SCC (top) and number of SCC tumors per mouse (bottom, $P < 0.05$ after week 19) seen in K14-*Angptl2* Tg mice administered normal ($n = 20$; red circles) or NAC-containing ($n = 28$; blue circles) water. C, comparison of the malignant conversion ratio of large papillomas to SCC in K14-*Angptl2* Tg mice provided normal versus NAC-treated water. D, Kaplan–Meier survival curves after initiation of chemical application of K14-*Angptl2* Tg mice provided normal ($n = 28$) or NAC-treated ($n = 27$) water ($P < 0.001$ by log-rank test).

NAC developed papillomas 3 weeks later than did Tg mice without NAC treatment (Fig. 3E, top), and the average number of large papillomas decreased to 0.35-fold that seen in NAC-treated Tg mice (Fig. 3E, bottom). In addition, we performed the same experiments in wild-type mice and confirmed the tumor-inhibitory effect of NAC (Supplementary Fig. S2).

Interestingly, we observed no difference in the ratio of large to total papillomas between mice treated with or without NAC (Fig. 3F), whereas SCC formation was significantly attenuated in NAC-treated versus untreated Tg mice (compare right with left images in Fig. 4A). By 30 weeks after initiation of chemical treatment, 100% of K14-*Angptl2* Tg without NAC treatment had developed malignant SCC, a condition seen in only 50% of NAC-treated mice (Fig. 4B, top). The average number of SCC tumors in NAC-treated K14-*Angptl2* Tg decreased to 0.15-fold relative to untreated Tg mice (Fig. 4B, bottom). The malignant conversion rate, defined as the ratio of the number of SCCs to the number of large papillomas (7, 26, 27), in NAC-treated K14-*Angptl2* Tg mice was lower than that in Tg mice without NAC treatment (Fig. 4C). In addition, survival of NAC-treated Tg mice was significantly prolonged relative to untreated Tg mice (Fig. 4D). Taken together, these results suggest that increased susceptibility to chemically induced skin carcinogenesis seen in this model is attributable to increased ROS production in skin tissues promoted by *Angptl2* overexpression.

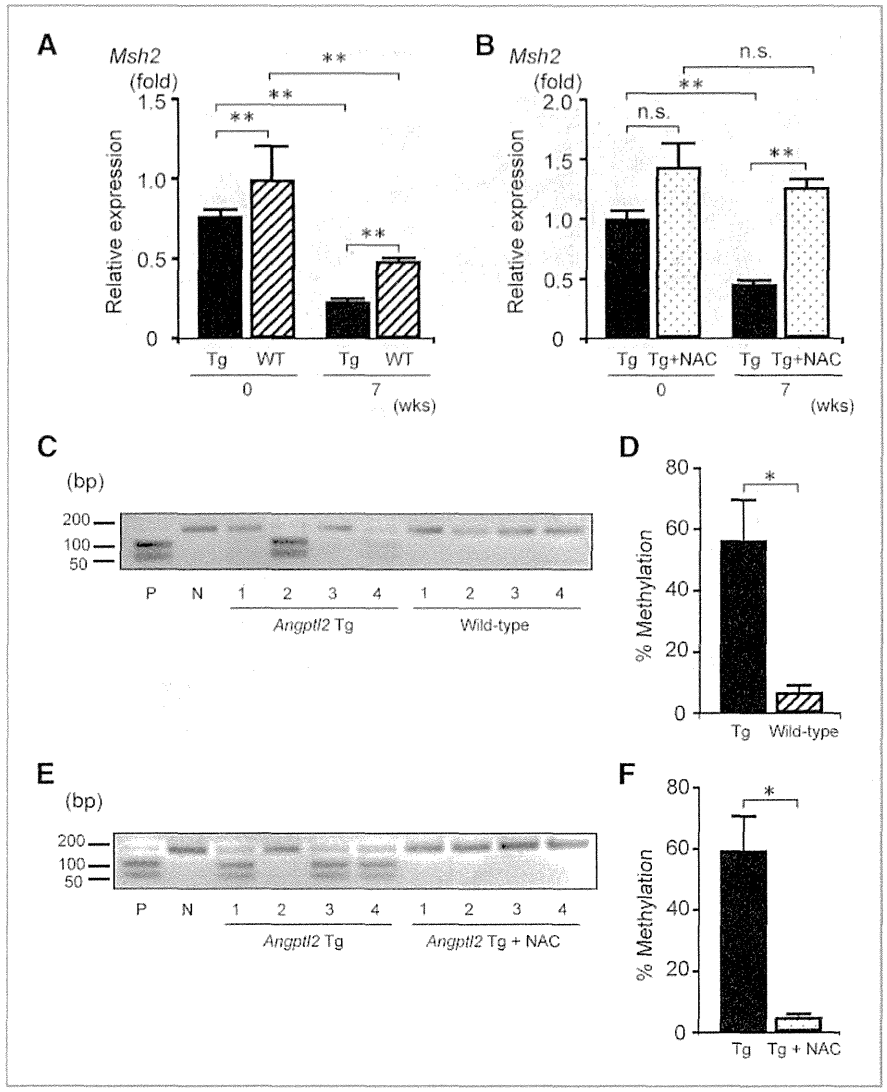

Figure 5. *Angptl2*-dependent hypermethylation of the *Msh2* promoter is ameliorated by antioxidant treatment. A and B, comparative expression levels of *Msh2* in skin tissues ($n = 7$) following a single application of DMBA plus 0 or 7 applications of PMA in K14-*Angptl2* Tg (Tg) versus wild-type (WT) mice (A), and between Tg mice provided normal (Tg) or NAC-treated (Tg + NAC) water (B). Values from wild-type or K14-*Angptl2* Tg without NAC treatment at week 0 data were set at 1. Data are expressed as mean ± SEM. **, $P < 0.01$; n.s., not statistically significant. C and E, representative COBRA methylation analysis following a single application of DMBA plus 7 applications of PMA to skin tissues of K14-*Angptl2* Tg or wild-type mice (C), and to K14-*Angptl2* Tg mice provided normal (*Angptl2* Tg) or NAC-treated (*Angptl2* Tg + NAC) water (E). CpG-methylated NIH 3T3 mouse genomic DNA served as a positive control (P). NIH 3T3 mouse genomic DNA served as a negative control (N). D and F, methylation percentage seen in K14-*Angptl2* Tg ($n = 7$) or wild-type ($n = 7$) mice (D), and in K14-*Angptl2* Tg mice provided normal (*Angptl2* Tg) ($n = 10$) or NAC-treated (*Angptl2* Tg + NAC) water ($n = 10$) (F). Data are expressed as mean ± SEM. **, $P < 0.01$ compared with wild-type mice.

Decreased *Msh2* mRNA levels in skin tissues of K14-*Angptl2* Tg mice are ameliorated by NAC treatment

Because inflammation and oxidative stress downregulate DNA-repair MMR proteins (28, 29), we used quantitative real-time PCR to determine whether Angptl2 alters the expression of *Msh2*, which encodes a MMR protein. *Msh2* expression level assessed prior to oncogenic chemical treatment differed in skin tissues of wild-type and K14-*Angptl2* Tg mice (Fig. 5A). By 7 weeks after initiation of chemical application, *Msh2* expression levels decreased in skin tissues of both K14-*Angptl2* Tg and wild-type mice, although that decrease was significantly greater in tissues from Tg mice (Fig. 5A). In addition, we found that Msh2 expression in skin did not decrease in *Angptl2* KO mice following chemical treatment (Supplementary Fig. S3).

Other DNA repair pathways such as nonhomologous end joining and homologous recombination could underlie rescue of DNA damage in chemical skin carcinogenesis. Therefore, we undertook Western blot analysis to assess levels of DNA-repair enzymes such as Atm and Atr (double- or single-strand breaks), Ku-70, and Ku-80 (nonhomologous end joining), and Rad51 and Brca2 (homologous recombination) in skin of wild-type, K14-*Angptl2*, and *Angptl2* KO mice. We found that, except for Msh2, expression levels of almost all of these factors were similar between wild-type and *Angptl2* KO mice or between *Angptl2* Tg and wild-type mice (Supplementary Figs S4 and S5). These results suggest that the Angptl2-induced decrease in Msh2 protein levels likely plays an important role in carcinogenesis.

Next, we examined whether decreased *Msh2* expression levels seen in K14-*Angptl2* Tg were attributable to increased ROS production in skin tissues. As noted, at 7 weeks after initiation of chemical application, *Msh2* expression levels in skin tissues of K14-*Angptl2* Tg mice had significantly

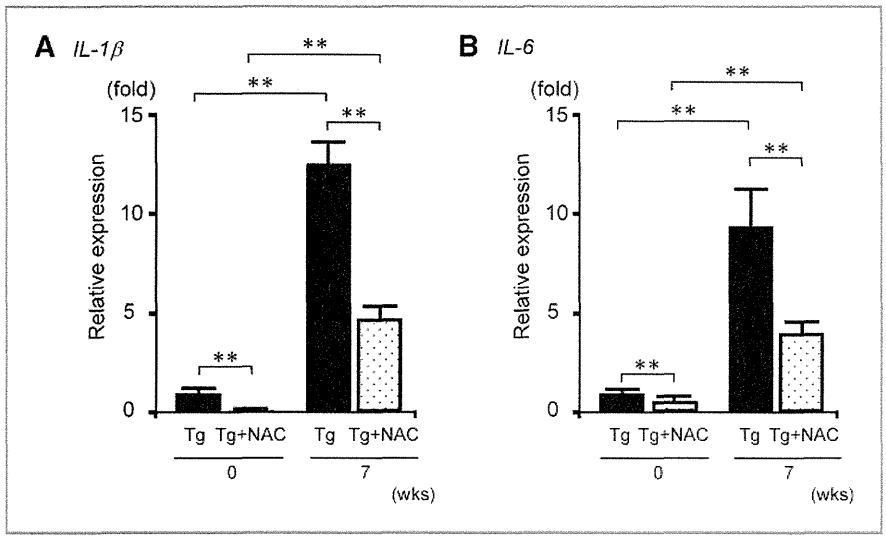

Figure 6. NAC treatment suppresses IL-1β and IL-6 expression in skin tissues following chemical treatment. A and B, comparative expression levels of IL-1β (A) and IL-6 (B) ($n = 7$) after a single application of DMBA plus 0 or 7 applications of PMA to skin tissues of K14-*Angptl2* Tg mice provided normal (Tg) or NAC-treated (Tg + NAC) water. Values from K14-*Angptl2* Tg without NAC treatment at week 0 data were set at 1. Data are expressed as mean ± SEM. **, $P < 0.01$.

decreased, whereas those decreases were ameliorated in Tg mice treated with NAC (Fig. 5B; Supplementary Fig. S6). Protein levels of DNA repair enzymes, except Msh2, were unchanged by NAC treatment (Supplementary Fig. S6). In addition, NAC treatment itself did not increase *Msh2* transcript levels (Supplementary Fig. S7), and decreased *Msh2* expression was ameliorated by NAC treatment of both wild-type and K14-*Angptl2* Tg mice at 7 weeks after initiation of chemical application (Fig. 5B; Supplementary Fig. S7). We conclude that high Angptl2 levels may suppress *Msh2* expression in skin tissues by increasing ROS production.

Methylation of the *Msh2* promoter in skin tissues of K14-*Angptl2* Tg mice decreases following NAC treatment

Oxidative stress has been associated with epigenetic modifications (30–32). Therefore, we asked whether decreased *Msh2* expression seen in skin tissues of K14-*Angptl2* Tg mice was due to oxidative stress and subsequent epigenetic modification of *Msh2*. To do so, we analyzed *Msh2* promoter methylation using COBRA, which provides reliable quantitative results across several DNA methylation levels (17, 33–35). Analysis of restriction digestion patterns of genomic DNA isolated from skin tissues of K14-*Angptl2* Tg mice indicated increased methylation frequency at the *Msh2* promoter, relative to levels seen in wild-type mice (Fig. 5C). Quantitative analysis revealed that approximately 60% of tissue samples from K14-*Angptl2* Tg mice showed high *Msh2* promoter methylation, whereas those levels at the same region of the promoter were seen in only 6.9% of tissue samples from wild-type mice (Fig. 5D). Representative data shown in Fig. 5E indicates that *Msh2* promoter methylation was significantly ameliorated by NAC treatment. Quantitative analysis revealed that NAC treatment decreased *Msh2* promoter methylation in skin tissues of K14-*Angptl2* Tg mice (Fig. 5F) to levels indistinguishable from those seen in wild-type mice (Fig. 5D). We conclude that decreased *Msh2* mRNA expression in skin tissues of K14-*Angptl2* Tg mice is likely attributable to Angptl2-induced oxidative stress and resultant increased *Msh2* promoter methylation.

NAC treatment attenuates Angptl2-induced skin tissue inflammation in a chemically induced SCC model

We previously reported that, based on levels of the proinflammatory factors interleukin (IL)-1β and IL-6, *Angptl2* expression levels in skin tissue are correlated with skin tissue inflammatory status in chemically induced SCC (7). Therefore, we asked whether NAC treatment altered IL-1β and IL-6 expression levels. IL-1β and IL-6 expression was significantly lower in the skin of NAC-treated compared with untreated Tg mice before chemical application (Fig. 6). These findings suggest that NAC treatment decreases inflammation in skin tissues of Tg mice by suppressing ROS production, and that Angptl2-induced inflammation is enhanced by oxidative stress.

MSH2 levels are inversely correlated with ANGPTL2 expression in UV-exposed human skin tissues

Finally, we examined ANGPTL2 and MSH2 expression in UV-exposed human skin tissues. We found that ANGPTL2 expression was low, whereas MSH2 expression was robust in normal skin tissues with minimal sun exposure (Fig. 7A). Although ANGPTL2 expression fluctuated somewhat in cases of actinic keratosis, MSH2 expression was inversely correlated with ANGPTL2 expression (Fig. 7B; Supplementary Fig. S8). In addition, ANGPTL2 expression was robust and MSH2 expression was weak in tissue of sun-exposed squamous cell carcinoma (Fig. 7C). These results suggest that UV exposure induces ANGPTL2 expression, leading to decreases MSH2 levels in human skin tissues.

Discussion

Our previous findings that K14-*Angptl2* Tg mice do not show papillomas or carcinomas when mice are treated with a tumor promoter (PMA) alone (7) indicate that Angptl2 is not an oncogene. However, we concluded that increased

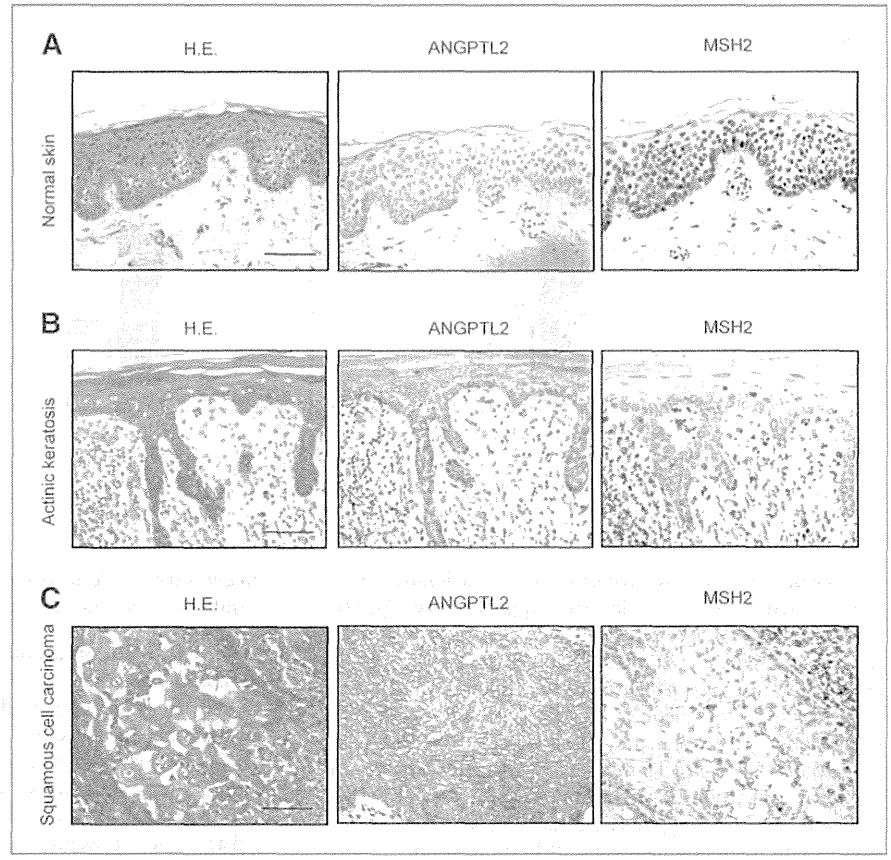

Figure 7. ANGPTL2 and MSH2 expression levels in normal skin, actinic keratosis, and squamous cell carcinoma. A–C, representative photographs of hematoxylin and eosin staining and immunohistochemical analysis with ANGPTL2 and MSH2 antibodies in normal human abdominal skin (non–sun-exposed area) (A), actinic keratosis on the face (sun-exposed area) (B), and SCC on the face (sun-exposed area) (C). Scale bars, 500 μm.

Angptl2 expression in skin tissue increases inflammation and accelerates carcinogenesis by enhancing susceptibility to both "pre-neoplastic change" and "malignant conversion." Our conclusion was based on studies using a skin carcinogenesis mice model employing DMBA/PMA treatment (7), a well-characterized model in which an initiating oncogenic mutation is followed by accumulation of additional oncogenic mutations (8–10). Findings reported here suggest that Angptl2 expression induces skin inflammation and likely accelerates acquisition of oncogenic mutations resulting in carcinogenesis. In addition, we find that in skin tissues Angptl2 overexpression correlates with decreased *Msh2* expression, likely due to methylation of its promoter region triggered by ROS accumulation in those tissues. Conversely, we show that continuous treatment with the antioxidant NAC reduces ROS accumulation in skin tissues and ameliorates decreased *Msh2* expression due to epigenetic modification, decreasing susceptibility to carcinogenesis. Finally, we report that antioxidant treatment also decreases skin tissue inflammation in K14-*Angptl2* Tg mice by suppressing ROS production, suggesting that Angptl2-induced inflammation is enhanced under oxidative stress conditions. Overall, we conclude that enhanced oxidative stress and chronic inflammation induced by Angptl2 synergize to increase susceptibility for carcinogenesis.

Currently, we do not know the mechanism underlying enhanced ROS production in skin tissue expressing excess Angptl2. Our previous report showing chronic inflammation in skin tissue of K14-*Angptl2* Tg mice demonstrated infiltration of skin tissue by inflammatory cells, including activated macrophages and neutrophils (7), both of which are sources of ROS (36). Angptl2 reportedly activates NF-κB proinflammatory signaling in various cell types (3–7, 37), which also enhances ROS production (38). Taken together, Angptl2 secreted from skin tissue of K14-*Angptl2* Tg mice may increase ROS production due to activity of infiltrated and activated inflammatory cells.

In addition, we demonstrate here decreased *Msh2* expression in skin tissues of K14-*Angptl2* Tg mice, most likely due to methylation of the *Msh2* promoter, an activity significantly improved by NAC treatment. Thus increased oxidative stress caused by *Angptl2* overexpression may promote *Msh2* promoter methylation. Previously, others have reported that ROS promotes development of human carcinogenesis through epigenetic regulation of gene expression (32). For example, ROS-induced oxidative stress reportedly silences promoters of tumor suppressors via hypermethylation (39). In addition, ROS induces Snail, which activates histone deacetylase 1 and DNA methyltransferase 1 (40). Moreover, we have

reported induction of an epithelial-to-mesenchymal transition (EMT) by increasing *Snail* mRNA expression and activating the TGF-β pathway in SCC of K14-*Angptl2* Tg mice (7), suggesting that Snail functions in *Msh2* promoter methylation. Further, ROS promotes phosphorylation of the transcription factors c-Jun and ATF2, increasing expression of their target genes (41). Interestingly, we reported that c-Jun and ATF2 activity increases Angptl2 expression (6), suggesting a mechanism through which ROS might increase Angptl2 expression.

We conclude that Angptl2 accelerates susceptibility to both "preneoplastic change" and "malignant conversion" by activating a cycle of chronic Inflammation and oxidative stress in the premalignant tissue microenvironment (Supplementary Fig. S9). More recently, we observed that spontaneous carcinogenesis is significantly decreased in *Angptl2* KO compared with wild-type mice (our unpublished data), suggesting that Angptl2 contributes not only to chemically induced carcinogenesis but also to various types of spontaneous cancers. Overall, our findings suggest that Angptl2 represents a target to develop new strategies to antagonize these activities in premalignant tissue.

Disclosure of Potential Conflicts of Interest

No potential conflicts of interest were disclosed.

Authors' Contributions

Conception and design: J. Aoi, M. Endo, H. Ihn, Y. Oike
Development of methodology: M. Endo, K. Miyata, H. Horiguchi, S. Hirakawa, H. Ihn
Acquisition of data (provided animals, acquired and managed patients, provided facilities, etc.): J. Aoi, M. Endo, A. Ogata
Analysis and interpretation of data (e.g., statistical analysis, biostatistics, computational analysis): J. Aoi, M. Endo, T. Kadomatsu, T. Masuda, S. Hirakawa, H. Ihn,
Writing, review, and/or revision of the manuscript: J. Aoi, M. Endo, S. Fukushima, S. Hirakawa, T. Sawa, H. Ihn, Y. Oike
Administrative, technical, or material support (i.e., reporting or organizing data, constructing databases): M. Endo, H. Odagiri, S. Fukushima, M. Jinnin, T. Akaike
Study supervision: M. Endo, K. Miyata, S. Fukushima, S. Hirakawa, H. Ihn, Y. Oike

Acknowledgments

The authors thank S. Iwaki, Y. Indoh, R. Shindo, and M. Nakata for providing technical assistance.

Grant Support

This work was financially supported by Grants-in-Aid for Scientific Research on Priority Areas from the Ministry of Education, Culture, Sports, Science and Technology of Japan, by the Japan Society for the Promotion of Science (JSPS) through its Funding Program for Next Generation World-Leading Researchers (NEXT Program), and a research program of the Project for Development of Innovative Research on Cancer Therapeutics (P-Direct), Ministry of Education, Culture, Sports, Science and Technology of Japan, and the Core Research for Evolutional Science and Technology (CREST) program of Japan Science and Technology Agency (JST), and by grants from the Takeda Science Foundation and the Yasuda Medical Foundation.

The costs of publication of this article were defrayed in part by the payment of page charges. This article must therefore be hereby marked *advertisement* in accordance with 18 U.S.C. Section 1734 solely to indicate this fact.

Received June 27, 2013; revised October 7, 2013; accepted October 28, 2013; published OnlineFirst November 20, 2013.

References

1. Balkwill F, Mantovani A. Inflammation and cancer: back to Virchow? Lancet 2001;357:539–45.
2. Mantovani A, Allavena P, Sica A, Balkwill F. Cancer-related inflammation. Nature 2008;454:436–44.
3. Tabata M, Kadomatsu T, Fukuhara S, Miyata K, Ito Y, Endo M, et al. Angiopoietin-like protein 2 promotes chronic adipose tissue inflammation and obesity-related systemic insulin resistance. Cell Metab 2009;10:178–88.
4. Okada T, Tsukano H, Endo M, Tabata M, Miyata K, Kadomatsu T, et al. Synoviocyte-derived angiopoietin-like protein 2 contributes to synovial chronic inflammation in rheumatoid arthritis. Am J Pathol 2010; 176:2309–19.
5. Ogata A, Endo M, Aoi J, Takahashi O, Kadomatsu T, Miyata K, et al. The role of angiopoietin-like protein 2 in pathogenesis of dermatomyositis. Biochem Biophys Res Commun 2012;418:494–9.
6. Endo M, Nakano M, Kadomatsu T, Fukuhara S, Kuroda H, Mikami S, et al. Tumor cell-derived angiopoietin-like protein ANGPTL2 is a critical driver of metastasis. Cancer Res 2012;72:1784–94.
7. Aoi J, Endo M, Kadomatsu T, Miyata K, Nakano M, Horiguchi H, et al. Angiopoietin-like protein 2 is an important facilitator of inflammatory carcinogenesis and metastasis. Cancer Res 2011;71: 7502–12.
8. Knudson AG. Two genetic hits (more or less) to cancer. Nat Rev Cancer 2001;1:157–62.
9. Hanahan D, Weinberg RA. Hallmarks of cancer: the next generation. Cell 2011;144:646–74.
10. Fearon ER, Vogelstein B. A genetic model for colorectal tumorigenesis. Cell 1990;61:759–67.
11. Glickman BW, Radman M. Escherichia coli mutator mutants deficient in methylation-instructed DNA mismatch correction. Proc Natl Acad Sci U S A 1980;77:1063–7.
12. Radman M, Wagner R. Mismatch repair in Escherichia coli. Annu Rev Genet 1986;20:523–38.
13. Modrich P. Methyl-directed DNA mismatch correction. J Biol Chem 1989;264:6597–600.
14. Modrich P, Lahue R. Mismatch repair in replication fidelity, genetic recombination, and cancer biology. Annu Rev Biochem 1996;65: 101–33.
15. Jun SH, Kim TG, Ban C. DNA mismatch repair system. Classical and fresh roles. FEBS J 2006;273:1609–19.
16. Umar A, Boland CR, Terdiman JP, Syngal S, de la Chapelle A, Rüschoff J, et al. Revised Bethesda Guidelines for hereditary nonpolyposis colorectal cancer (Lynch syndrome) and microsatellite instability. J Natl Cancer Inst 2004;96:261–8.
17. Conde-Perezprina JC, Luna-Lopez A, Lopez-Diazguerrero NE, Damian-Matsumura P, Zentella A, Konigsberg M. Msh2 promoter region hypermethylation as a marker of aging-related deterioration in old retired female breeder mice. Biogerontology 2008;9:325–34.
18. Harfe BD, Jinks-Robertson S. Sequence composition and context effects on the generation and repair of frameshift intermediates in mononucleotide runs in Saccharomyces cerevisiae. Genetics 2000; 156:571–8.
19. Campbell MR, Wang Y, Andrew SE, Liu Y. Msh2 deficiency leads to chromosomal abnormalities, centrosome amplification, and telomere capping defect. Oncogene 2006;25:2531–6.
20. Hawighorst T, Oura H, Streit M, Janes L, Nguyen L, Brown LF, et al. Thrombospondin-1 selectively inhibits early-stage carcinogenesis and angiogenesis but not tumor lymphangiogenesis and lymphatic metastasis in transgenic mice. Oncogene 2002;21:7945–56.
21. Hawighorst T, Velasco P, Streit M, Hong YK, Kyriakides TR, Brown LF, et al. Thrombospondin-2 plays a protective role in multistep carcinogenesis: a novel host anti-tumor defense mechanism. EMBO J 2001; 20:2631–40.
22. Kirkham N. Tumors and Cysts of the Epidermis. In: David E., Elder, et al. editors. Lever's Histopathology of the Skin. Philadelphia: Lippincott Williams & Wilkins; 2009. p. 791–849.

23. Garcia-Manero G, Daniel J, Smith TL, Kornblau SM, Lee MS, Kantarjian HM, et al. DNA methylation of multiple promoter-associated CpG islands in adult acute lymphocytic leukemia. Clin Cancer Res 2002; 8:2217–24.
24. Uchida K. 4-Hydroxy-2-nonenal: a product and mediator of oxidative stress. Prog Lipid Res 2003;42:318–43.
25. Yano M, Watanabe K, Yamamoto T, Ikeda K, Senokuchi T, Lu M, et al. Mitochondrial dysfunction and increased reactive oxygen species impair insulin secretion in sphingomyelin synthase 1-null mice. J Biol Chem 2011;286:3992–4002.
26. Hirakawa S, Brown LF, Kodama S, Paavonen K, Alitalo K, Detmar M. VEGF-C-induced lymphangiogenesis in sentinel lymph nodes promotes tumor metastasis to distant sites. Blood 2007;109:1010–7.
27. Hirakawa S, Kodama S, Kunstfeld R, Kajiya K, Brown LF, Detmar M. VEGF-A induces tumor and sentinel lymph node lymphangiogenesis and promotes lymphatic metastasis. J Exp Med 2005;201:1089–99.
28. Colotta F, Allavena P, Sica A, Garlanda C, Mantovani A. Cancer-related inflammation, the seventh hallmark of cancer: links to genetic instability. Carcinogenesis 2009;30:1073–81.
29. Hsu T, Huang KM, Tsai HT, Sung ST, Ho TN. Cadmium(Cd)-induced oxidative stress down-regulates the gene expression of DNA mismatch recognition proteins MutS homolog 2 (MSH2) and MSH6 in zebrafish (Danio rerio) embryos. Aquat Toxicol 2013;126:9–16.
30. Grivennikov SI, Greten FR, Karin M. Immunity, inflammation, and cancer. Cell 2010;140:883–99.
31. Valko M, Rhodes CJ, Moncol J, Izakovic M, Mazur M. Free radicals, metals and antioxidants in oxidative stress-induced cancer. Chem Biol Interact 2006;160:1–40.
32. Campos AC, Molognoni F, Melo FH, Galdieri LC, Carneiro CR, D'Almeida V, et al. Oxidative stress modulates DNA methylation during melanocyte anchorage blockade associated with malignant transformation. Neoplasia 2007;9:1111–21.
33. Xiong Z, Laird PW. COBRA: a sensitive and quantitative DNA methylation assay. Nucleic Acids Res 1997;25:2532–4.
34. Grunau C, Sanchez C, Ehrlich M, van der Bruggen P, Hindermann W, Rodriguez C, et al. Frequent DNA hypomethylation of human juxtacentromeric BAGE loci in cancer. Genes Chromosomes Cancer 2005;43:11–24.
35. Goldberg M, Rummelt C, Laerm A, Helmbold P, Holbach LM, Ballhausen WG. Epigenetic silencing contributes to frequent loss of the fragile histidine triad tumour suppressor in basal cell carcinomas. Br J Dermatol 2006;155:1154–8.
36. Klaunig JE, Kamendulis LM. The role of oxidative stress in carcinogenesis. Annu Rev Pharmacol Toxicol 2004;44:239–67.
37. Tazume H, Miyata K, Tian Z, Endo M, Horiguchi H, Takahashi O, et al. Macrophage-derived angiopoietin-like protein 2 accelerates development of abdominal aortic aneurysm. Arterioscler Thromb Vasc Biol 2012;32:1400–9.
38. Kundu JK, Surh YJ. Inflammation: gearing the journey to cancer. Mutat Res 2008;659:15–30.
39. Ziech D, Franco R, Pappa A, Panayiotidis MI. Reactive oxygen species (ROS)–induced genetic and epigenetic alterations in human carcinogenesis. Mutat Res 2011;711:167–73.
40. Lim SO, Gu JM, Kim MS, Kim HS, Park YN, Park CK, et al. Epigenetic changes induced by reactive oxygen species in hepatocellular carcinoma: methylation of the E-cadherin promoter. Gastroenterology 2008;135:2128–40, 40 e1–8.
41. Klaunig JE, Wang Z, Pu X, Zhou S. Oxidative stress and oxidative damage in chemical carcinogenesis. Toxicol Appl Pharmacol 2011; 254:86–99.

Case Report

DOI: 10.5582/bst.8.64

A case of psoriasis accompanied by arthritis after delivery

Hisashi Kanemaru, Masatoshi Jinnin*, Kae Asao, Asako Ichihara, Katsunari Makino, Ikko Kajihara, Akihiko Fujisawa, Satoshi Fukushima, Hironobu Ihn

Department of Dermatology and Plastic Surgery, Faculty of Life Sciences, Kumamoto University, Honjo, Kumamoto, Japan.

Summary **Psoriasis and psoriatic arthritis are chronic inflammatory diseases of the skin and joints, but the relationship between them has not been fully understood. Since the delay of treatment for psoriatic arthritis can result in the severe deformities, it is important to identify the pathological triggers of the arthritis. On the other hand, many reports suggest that the changes of immune balance during pre/postpartum period are associated with the state of autoimmune diseases. Here, we report a female case with psoriasis whose arthritis may be triggered by the delivery. Our report suggests that immune tolerance may diminish in the postpartum period, which may alter the susceptibility to arthritis. Female patients should be followed-up carefully during postpartum period against the development of arthritis.**

Keywords: Autoimmune diseases, immune tolerance, psoriatic arthritis

1. Introduction

Psoriasis is a chronic inflammatory dermatosis of the skin affecting as many as 1-2% of Caucasian and 0.02-0.1% of Japanese people (*1*). Among them, some cases are thought to be accompanied with arthritis. Psoriatic arthritis is different from rheumatoid arthritis (RA) in terms of its predilection for the distal interphalangeal joints and negative rheumatoid factors (RF), and therefore is included in seronegative spondyloarthropathy. The arthritis is associated with cutaneous psoriasis in more than 90% of cases, and is preceded by the cutaneous lesion in 75% cases (*2*). Though treatment with monoclonal antibodies against tumor necrosis factor (TNF) (*e.g.* infliximab and adalimumab) or soluble TNF receptor (etanercept) have been in clinical use recently, the delay of treatment may result in the reduced quality of life and the severe deformities resembling the joint changes seen in RA. Therefore, the early detection and treatment of arthritis is necessary in psoriasis patients, and it is important to identify the pathological triggers of the arthritis. Until today, genetic factors, mechanical stimulations, infections, drugs, and immunologic factors are reported as triggers of psoriatic arthritis (*2*). Here, we report a female case with psoriasis whose arthritis may be triggered by the delivery.

**Address correspondence to:*
Dr. Masatoshi Jinnin, Department of Dermatology and Plastic Surgery, Faculty of Life Sciences, Kumamoto University, 1-1-1 Honjo, Kumamoto, Japan.
E-mail: mjin@kumamoto-u.ac.jp

2. Case reports

A 37-year-old Japanese female visited our hospital, for the treatment of the eruption and arthritis. There was no record of similar conditions in her family history. She had been diagnosed as having psoriasis vulgaris more than 20 years ago, and treated with corticosteroid ointments. She had never had arthralgia. She got her first child 3 months before the first visit, without any problems related to the delivery. However, she started to complain of arthralgia after the delivery, and the arthritis as well as the eruption worsened gradually. On physical examination, the patients had the skin lesions in the trunk and extremities. The each lesion was well-demarcated, erythematous plaque covered by silver-white scales (Figure 1). Neither pustules nor nail changes were observed. She could not stand up by herself because of her joint swelling and pain, which was present in finger, wrist, elbow, knee, and ankle joints.

As laboratory findings, the white blood cell (WBC) count and C-reactive protein (CRP) levels was slightly increased at 9,000/uL and 2.07 mg/dL, respectively. Antinuclear antibody or anti-cyclic citrullinated

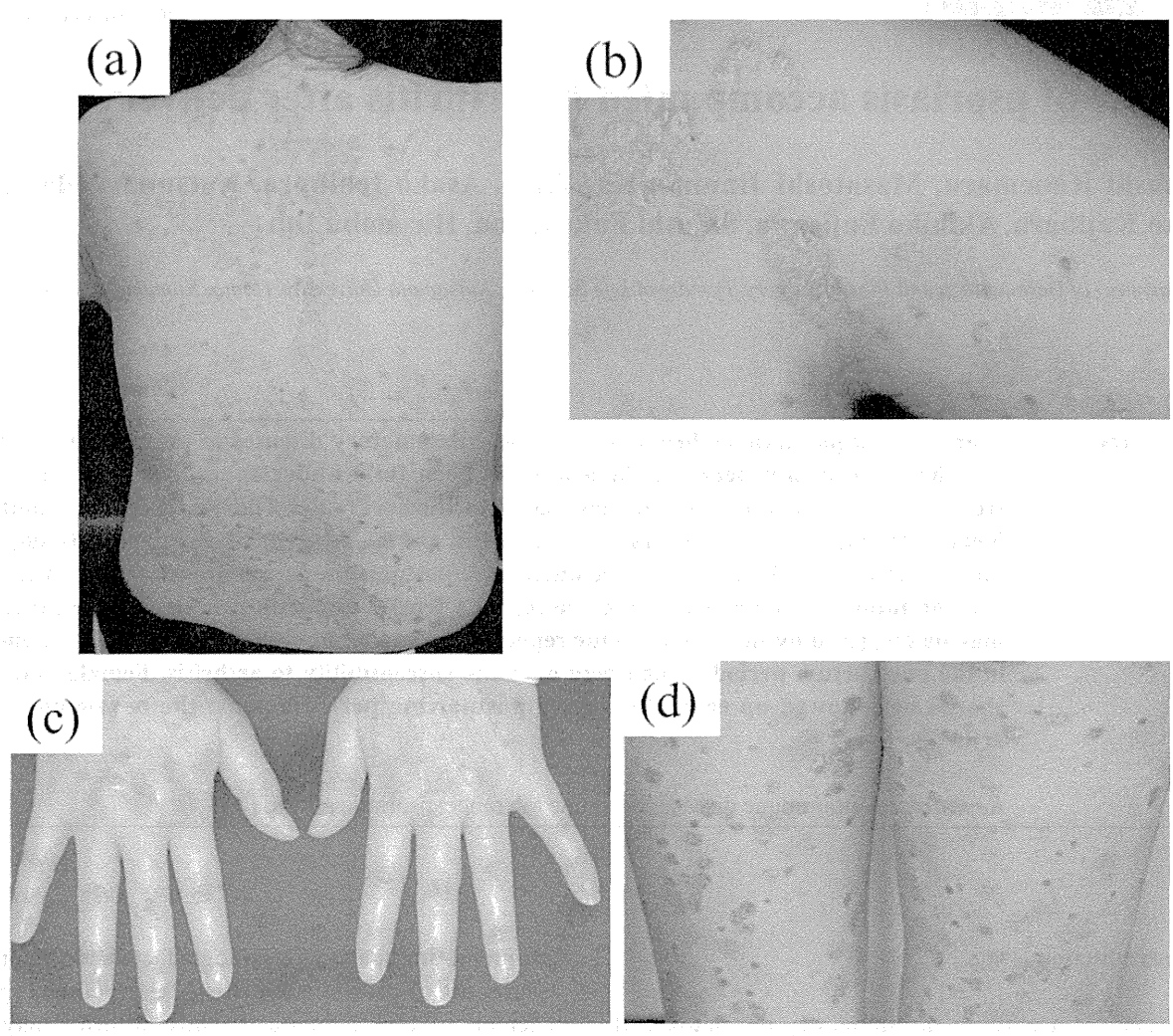

Figure 1. Well-demarcated, erythematous plaques covered by silver-white scales in the back (a), upper arm (b), hands (c), and thighs (d).

Figure 2. 99mTc-MDP bone scintigraphy showing the increased uptake in finger, wrist, elbow, knee, and ankle joints.

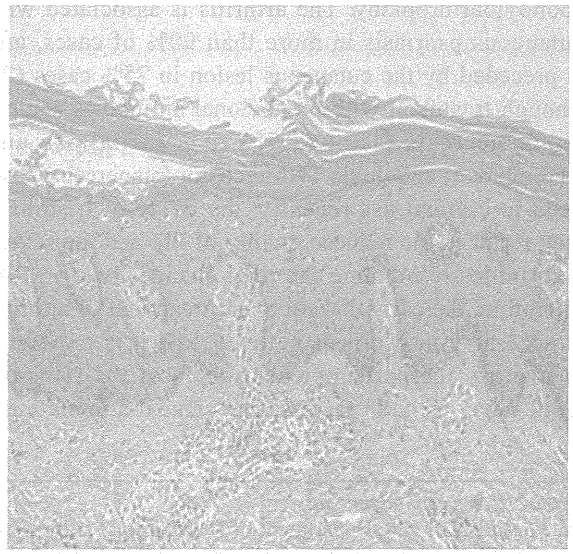

Figure 3. Haematoxylin and eosin (H&E) staining of biopsy specimen from cutaneous lesion.

peptide (CCP) antibody was not detected. RF was also negative (7 IU/mL, normally < 20 IU/mL), and the serum level of matrix metalloproteinase (MMP)-3 was not increased (32.1 ng/mL, normally < 59.7 ng/mL). Laboratory results of other blood cell counts, blood chemistry analysis (including serum albumin, p-glucose or HbA1c), urinalysis, and chest radiography were within normal limits. Bone scintigraphy showed increased uptake in multiple joints (Figure 2), which were identical to the swollen and painful joints.

A skin biopsy from the affected area revealed acanthosis, hypogranulosis and extensive overlying parakeratotic scale in the epidermis. Perivascular infiltration of neutrophils and lymphocytes in the dermis was also seen (Figure 3).

Based on the findings of blood examination, bone scintigram and skin biopsy, she was diagnosed as having psoriasis and postpartum development of arthritis. Her Psoriasis Area and Severity Index (PASI) of the cutaneous lesion, DAS28-CRP and visual analogue scale (VAS) of the arthritis was 22.6, 3.9, and 60, respectively.

The patient was treated with infliximab immediately. After three times of administration, her eruption and arthritis have disappeared completely (Figure 4). The PASI and VAS was also improved dramatically as shown in Figure 5.

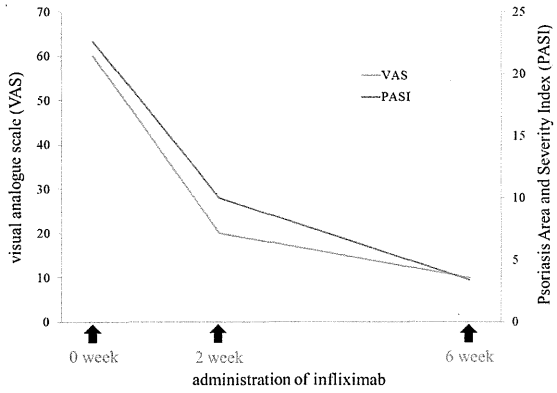

Figure 5. The time course of the changes of PASI of the cutaneous lesions and VAS of the arthritis during the treatment with infliximab, which was administered three times (0, second and, sixth week).

3. Discussion

Though the aetiology of psoriasis and psoriatic arthritis is multifactorial, one of the most likely pathogenic agents may be T cell (*2*). This suggestion is supported by many clinical studies for the treatment of psoriasis and psoriatic arthritis: e.g. the clinical efficacy of cyclosporin, a highly selective antagonist of T-cell proliferation and activation (*2*). Psoriasis has been regarded as the Th1-mediated disease like RA and Crohn disease (*2-5*). However, in the last few years, Th17, a new subset of CD4 T cells, has been identified, based on their production of IL-17 (*6*). There are many reports that indicate IL-17 is associated with the pathogenesis of psoriasis (*7*). In addition, it was reported that regulatory T cells (Treg), which suppress CD4 helper T cells, are impaired in many autoimmune diseases (*8*). Psoriatic Treg have also been found to defect the activity, which may result in the auto-reactive T cell activation and contribute to the pathogenesis for psoriasis (*9*). Taken together, in psoriasis and psoriatic arthritis, Th1 and Th17 should be predominant rather than Th2 and Treg, like RA.

On the other hand, although the change of immune system during pregnancy has not been fully clarified,

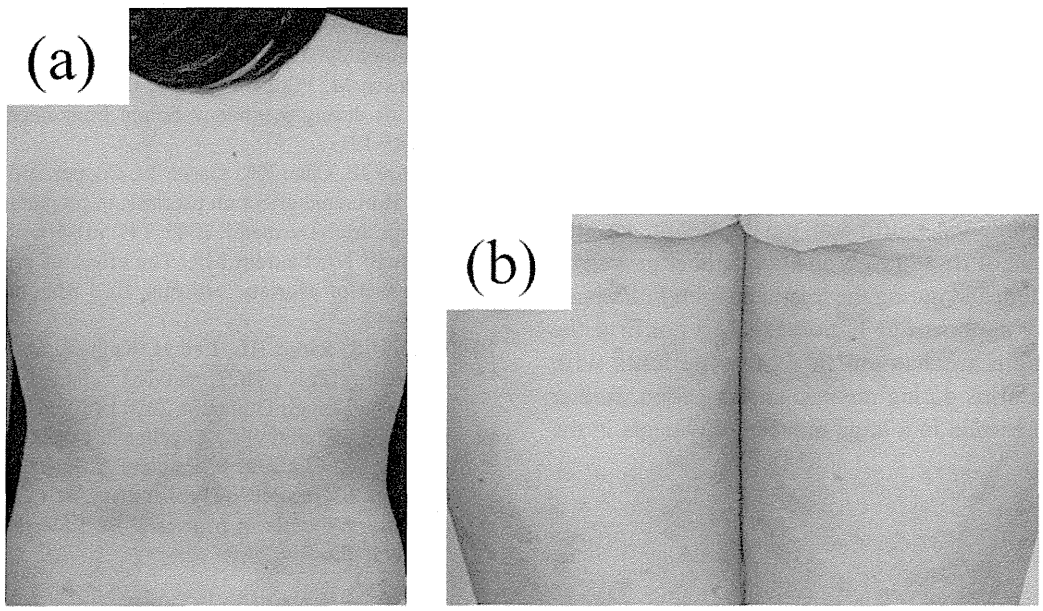

Figure 4. Macroscopic appearance of the back (a) and thighs (b) of the patient after three times of infliximab administration.

many studies have reported a predominant Th2/Treg-type immunity and a suppressed Th1/17-type immunity during normal pregnancy (*10*). These immunological changes seem to be necessary for successful pregnancy, because the predominance of Th1/17-type immunity over Th2/Treg-type immunity is observed in abortion patients (*10*). Estrogens and progesterone are known to inhibit Th1 immune responses including TNF-α and IL-12 production, while induce Th2 immune responses like IL-10 and IL-4 production (*11*). These hormones are significantly increased during pregnancy in comparison with the postpartum period. In addition, during pregnancy, Th1-type immunity is well controlled to avoid its overstimulation, probably due to the suppression by Treg, which are observed to increase in decidua (*11*). Furthermore, the level of IL-17 in normal pregnancy is lower than that in non-pregnancy, and Th17 is thought to be inhibited in the former condition (*12*). Taken together, in pregnancy, Th2/Treg-type immunity should be predominant over Th1/Th17-type immunity by the above changes in the hormones and cytokines, and the subsequent rebound of Th1/Th17 may occur after delivery.

The above notions suggest that immune tolerance may diminish in the postpartum period, which may alter the susceptibility to autoimmune diseases including RA. Actually, postpartum onset of RA by the Th1/Th17 activation has been well described (*13*). On the other hand, psoriasis is known to be one of the diseases which are improved during pregnancy (*14*). Furthermore, there is a very old report that states 6 of 20 psoriasis patients developed arthritis during postpartum period (*15*). Since then, however, there have been no reports describing similar cases. Our case is the second to suggest that the changes in immune balance after delivery may be the newly described trigger of arthritis in female patients with psoriasis. From this point of view, female patients should be followed-up carefully during postpartum period against the occurrence of arthritis.

Recent papers have shown that serum IL-17 level is reduced and Treg level is increased after infliximab treatment in psoriasis (*16,17*). As the limitation of the paper, because blood samples of the patient were not collected, we could not perform time course measurement of IL-17 levels and the number or activity of Treg before and during the treatment with infliximab, which may support our hypothesis. To confirm the immunologic mechanism in female patients with psoriatic arthritis during pre/postpartum period, further studies are needed in a large number of patients in the future.

References

1. Takahashi H, Nakamura K, Kaneko F, Nakagawa H, Iizuka H, Japanese Society for Psoriasis Research. Analysis of psoriasis patients registered with the Japanese Society for Psoriasis Research from 2002-2008. J Dermatol. 2011; 38:1125-1129.
2. Ciocon DH, Kimball AB. Psoriasis and psoriatic arthritis: separate or one and the same? Br J Dermatol. 2007; 157:850-860.
3. Jacob SE, Nassiri M, Kerdel FA, Vincek V. Simultaneous measurement of multiple Th1 and Th2 serum cytokines in psoriasis and correlation with disease severity. Mediators Inflamm. 2003; 12:309-313.
4. Berner B, Akça D, Jung T, Muller GA, Reuss-Borst MA. Analysis of Th1 and Th2 cytokines expressing CD4+ and CD8+ T cells in rheumatoid arthritis by flow cytometry. J Rheumatol. 2000; 27:1128-1135.
5. Parronchi P, Romagnani P, Annunziato F, Sampognaro S, Becchio A, Giannarini L, Maggi E, Pupilli C, Tonelli F, Romagnani S. Type 1 T-helper cell predominance and interleukin-12 expression in the gut of patients with Crohn's disease. Am J Pathol. 1997; 150:823-832.
6. Weaver CT, Harrington LE, Mangan PR, Gavrieli M, Murphy KM. Th17: An effector CD4 T cell lineage with regulatory T cell ties. Immunity. 2006; 24:677-688.
7. Li J, Li D, Tan Z. The expression of interleukin-17, interferon-γ, and macrophage inflammatory protein-3 α mRNA in patients with psoriasis vulgaris. J Huazhong Univ Sci Technolog Med Sci. 2004; 24:294-296.
8. Buckner JH. Mechanisms of impaired regulation by CD4(+)CD25(+)FOXP3(+) regulatory T cells in human autoimmune diseases. Nat Rev Immunol. 2010; 10:849-859.
9. Goodman WA, Cooper KD, McCormick TS. Regulation generation: The suppressive functions of human regulatory T cells. Crit Rev Immunol. 2012; 32:65-79.
10. Saito S, Nakashima A, Shima T, Ito M. Th1/Th2/Th17 and regulatory T-cell paradigm in pregnancy. Am J Reprod Immunol. 2010; 63:601-610.
11. Robinson DP, Klein SL. Pregnancy and pregnancy-associated hormones alter immune responses and disease pathogenesis. Horm Behav. 2012; 62:263-271.
12. Santner-Nanan B, Peek MJ, Khanam R, Richarts L, Zhu E, Fazekas de St Groth B, Nanan R. Systemic increase in the ratio between Foxp3+ and IL-17-producing CD4+ T cells in healthy pregnancy but not in preeclampsia. J Immunol. 2009; 183:7023-7030.
13. Ostensen M, Villiger PM. The remission of rheumatoid arthritis during pregnancy. Semin Immunopathol. 2007; 29:185-191.
14. Murase JE, Chan KK, Garite TJ, Cooper DM, Weinstein GD. Hormonal effect on psoriasis in pregnancy and post partum. Arch Dermatol. 2005; 141:601-606.
15. McHugh NJ, Laurent MR. The effect of pregnancy on the onset of psoriatic arthritis. Br J Rheumatol. 1989; 28:50-52.
16. Kagami S, Rizzo HL, Lee JJ, Koguchi Y, Blauvelt A. Circulating Th17, Th22, and Th1 cells are increased in psoriasis. J Invest Dermatol. 2010 ; 130:1373-1383.
17. Diluvio L, Romiti ML, Angelini F, Campione E, Rossi P, Prinz JC, Chimenti S, Lamioni A. Infliximab therapy induces increased polyclonality of CD4+CD25+ regulatory T cells in psoriasis. Br J Dermatol. 2010; 162:895-897.

(Received October 13, 2012; Revised December 30, 2013; Accepted January 31, 2014)

International Journal of
Dermatology

Report

MIRSNP rs2910164 of miR-146a is associated with the muscle involvement in polymyositis/dermatomyositis

Yoshifumi Okada, Masatoshi Jinnin, MD, PhD, Takamitsu Makino, MD, PhD, Ikko Kajihara, MD, PhD, Katsunari Makino, MD, PhD, Noritoshi Honda, MD, Wakana Nakayama, MD, Kuniko Inoue, MD, Satoshi Fukushima, MD, PhD, and Hironobu Ihn, MD, PhD

Department of Dermatology and Plastic Surgery, Faculty of Life Sciences, Kumamoto University, Kumamoto, Japan

Correspondence
Masatoshi Jinnin, MD, PHD
Department of Dermatology and Plastic Surgery, Faculty of Life Sciences
Kumamoto University
Honjo 1-1-1
Kumamoto 860-8556
Japan
E-mail: mjin@kumamoto-u.ac.jp

Conflicts of interest: The authors declare that they have no conflicts of interest that might influence the results and discussion in this paper.

Abstract

Background Recently, single nucleotide polymorphisms (SNPs) located in microRNAs, the so-called MIRSNPs, have attracted attention for their possible involvement in the pathogenesis of various diseases. Such MIRSNPs may have a functional role, due to the alteration of microRNA function, and can be a disease marker. In this study, we evaluated the possibility that MIRSNP rs2910164 in miR-146a can be a useful marker for the diagnosis and evaluation of disease activity of polymyositis/dermatomyositis (PM/DM).

Methods DNA was obtained from 25 patients with DM, 16 with clinically amyopathic DM, and three with PM, and genotyped by polymerase chain reaction (PCR). The PCR products were digested by *MnlI*, and the digested products were run out on a 3% agarose gel. Serum levels of miR-146a were measured by real-time PCR.

Results We could not find a significant difference in the frequency of genotype distribution between controls and patients with PM/DM. However, the frequency of muscle weakness and dysphagia in patients with CC genotype was significantly higher as compared with patients with CG or GG genotype. In addition, the minimum free energy between miR-146a and its complementary strand with G allele is estimated at −26.8 kcal/mol, while that of C allele is at −24.0 kcal/mol, suggesting that the MIRSNP rs2910164 is functional. Serum miR-146a levels tended to be decreased in patients with DM with the CC genotype.

Conclusions Taken together, miR-146a may be involved in the pathogenesis of PM/DM, and patients with the CC genotype are at higher risk of muscle involvement.

Introduction

Polymyositis/dermatomyositis (PM/DM) is a chronic idiopathic inflammatory disorder that may affect skeletal muscles, skin, lungs, or other organs. DM is distinguished from PM by the presence of cutaneous involvement such as heliotrope eyelids and Gottron's phenomenon. Patients with DM with clinically and histopathologically typical cutaneous lesions but without muscle involvement are diagnosed as clinically amyopathic DM (CADM).[1] Because this disease can overlap with other autoimmune disorders such as systemic lupus erythematosus, rheumatoid arthritis, and systemic sclerosis, the pathogenesis of PM/DM is thought to be mediated by autoimmunity. However, the exact cause of this disease is still to be clarified.

microRNAs (miRNAs), small noncoding RNAs on average only 22 nucleotides long, usually function as negative regulators of target mRNAs at the translational level by binding to 3′-untranslated region (UTR) of the target. In humans, there are thought to be more than a thousand miRNAs,[2] and each has been implicated in various cell functions, including immune response as well as cell development, differentiation, growth, or apoptosis. Accordingly, previous studies have indicated the possibility that miRNAs are involved in the pathogenesis of various diseases: Eisenberg *et al.*[3] already reported that expression of several miRNAs are up- or downregulated in muscle tissue of PM/DM compared with that of normal control muscle.

More recently, single nucleotide polymorphisms (SNPs) in miRNA target sites or in miRNAs themselves, so-called MIRSNPs, have attracted attention for their possible involvement in the pathogenesis of various disorders. Such MIRSNPs may have a functional role, by altering miRNA function, and can be a disease marker.[4–7] In this study, we investigate whether MIRSNP rs2910164 in miR-146a (one of the miRNAs implicated in various autoimmune diseases, including systemic lupus erythematosus or rheumatoid arthritis[8–10]) is involved in the pathogenesis of PM/DM.

International Journal of Dermatology 2014, **53**, 300–304

Patients and methods

Clinical assessment and patient's material

We collected skin samples from 41 patients with DM (16 men and 25 women) and three patients with PM (three women) when they were newly diagnosed according to the criteria of Bohan and Peter.[11,12] Among 41 DM, 16 patients with clinically and histopathologically typical cutaneous lesions but without myositis were diagnosed as CADM according to previous criteria.[1] At the time of skin sampling, patients had received no treatments, including steroids, azathioprine, and methotrexate. Manual muscle testing was used to evaluate muscle weakness. They were reviewed by two independent observers who were unaware of the clinical condition. Electromyographic examination and biopsies of muscle were performed at the time of diagnosis. Lung involvement was diagnosed based on the findings of chest radiography, computed tomography of the chest, and lung function tests. Skin samples were also collected from 107 controls. Institutional review board approval and written informed consent were obtained before patients and healthy volunteers were entered into this study according to the Declaration of Helsinki.

DNA extraction

DNA extraction from skin samples was performed with TaKaRa DEXPAT® (Takara Bio Inc., Shiga, Japan). Frozen sections (20 μm thick) were collected in 1.5 mm tubes and 250 μL of DEXPAT preheated at 100 °C was added to the sections. The samples were incubated at 100 °C for an additional 10 minutes. After the centrifuge at maximum speed, 120 μL of supernatant containing genomic DNA was collected.

Polymerase chain reaction for single nucleotide polymorphism analysis

The primer pair used for PCR were: forward: GTATC CTCAGCTTTGAGAACT, reverse: CTCACA GGAACTCACACTC. The primer set was prevalidated to generate single amplicon. Two microliters of genomic DNA was used as template for amplification in a 20 μl reaction solution containing 10 μl of SYBR Premix Ex Taq™ II (Takara Bio Inc.), 0.5 μl of each primer, and 2 μl of dimethyl sulfoxide. PCR was performed for 40 cycles of denaturation for five seconds at 95 °C, annealing for 10 seconds at 58 °C, and extension for 20 seconds at 72 °C.

Restriction enzyme reaction and gel electrophoresis

Polymerase chain reaction product (10 μL) is used for the digestion by *Mnl*I (New England Biolab, Ipswich, MA, USA) in a 15 μL reaction containing 1.5 μL of 10× buffer 4, 0.15 μL of 100× BSA, and 0.3 μL of the enzyme. The mixture was incubated at 37 °C overnight. The digested products were run out on a 3% agarose gel containing ethidium bromide.

miRNA extraction from serum and polymerase chain reaction analysis of miRNA expression

miRNA isolation from serum samples was performed with miRNeasy RNA isolation kit (Qiagen, Valencia, CA, USA) following the manufacturer's instructions with minor modification.[13,14] Briefly, 100 μL of serum were supplemented with 5 μL of 5 fmol/μL synthetic nonhuman miRNA (Caenorhabditis elegans miR-54; Takara Bio Inc.) as controls providing an internal reference for normalization of technical variations between samples.

cDNA was synthesized from the miRNA with Mir-X miRNA First Strand Synthesis and SYBR qRT-PCR Kit (Takara Bio Inc.). Quantitative real-time PCR used primers for miR-146a or cel-miR-54 (Takara Bio Inc.) and templates mixed with the SYBR Premix. DNA was amplified for 40 cycles of denaturation for five seconds at 95 °C and annealing for 20 seconds at 60 °C. Transcript level of miR-146a was normalized to that of cel-miR-54 in the same sample.

Results

Genotyping

The miR-146a C/G polymorphism (rs2910164) was genotyped with PCR. The amplified fragment contains miR-146a gene SNP site encoding either the nucleotide G (allele G) or C (allele C) that results in the creation of a *Mnl*I restriction enzyme site. Three products (126, 77, and 15 bp) were observed if the PCR amplicon contains

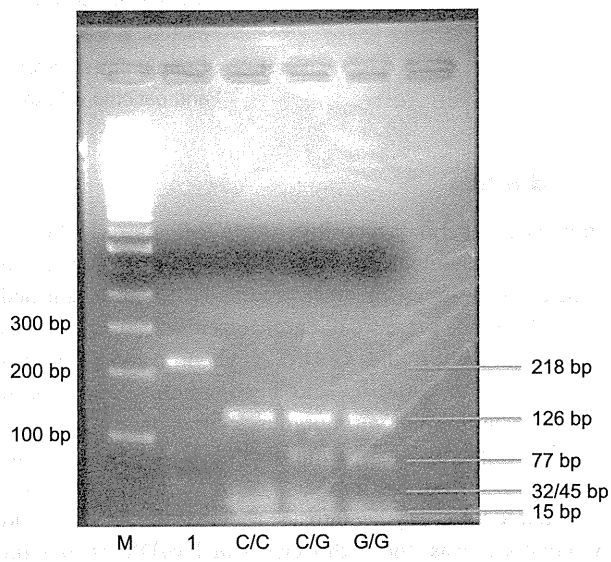

Figure 1 3% agarose gel showing the different genotypes for the miR-146 C/G polymorphism. *Lane M*, 100 bp marker; *lane 1*, polymerase chain reaction product (218 bp band); *lane 2*, CC genotype (15, 32, 45, and 126 bp bands); *lane 3*, CG genotype (15, 32, 45, 77, and 126 bp bands); *lane 4*, GG genotype (15, 77, and 126 bp bands)

allele G and four products (126, 45, 32, and 15 bp) in case of allele C (Fig. 1).

The frequencies of genotype and allele at rs2910164 in patients with polymyositis/dermatomyositis

The frequencies of genotype at the SNP site are listed in Table 1. In 107 controls, genotype distribution was 51 CC (47.7%), 53 CG (49.5%), and three GG (2.8%), which are similar to previous reports in an Asian population (see dbSNP; http://www.ncbi.nlm.nih.gov/projects/SNP/snp_ref.cgi?rs=rs2910164). On the other hand, when 41 patients with PM/DM were evaluated, the genotype distribution was 15 CC (34.1%), 29 CG (65.9%), and no GG; CG genotype tended to be increased in patients with PM/DM but was not statistically significant ($P = 0.13$, Table 1). Similarly, distribution analysis of C allele and G allele resulted in no significant difference between controls and patients with PM/DM ($P = 0.35$, Table 2). Furthermore, we could not find significant difference in the genotype distribution or allele frequency among patients with DM, CADM, and PM, and controls.

However, as shown in Table 3, among 25 patients with DM, the comparison of clinical and laboratory features between genotypes of miR-146a SNP revealed that the prevalence of muscle weakness in patients with CC genotype was significantly higher compared to patients with CG or GG genotype (100.0% vs. 62.5%, $P < 0.05$). The frequency of dysphagia was also significantly increased in patients with CC genotype than those without (66.7% vs. 9.1%, $P < 0.01$). However, there was no significant difference between these groups in terms of findings on electromyographic examination, histology, including intensity of inflammation and degree of fiber degeneration, or other clinical parameters, including pulmonary function tests and chest radiograph.

On the other hand, because no patients with CADM had muscle weakness and dysphagia (Table 4), no difference was found in the other clinical and laboratory findings between patients with CC genotype and those with CG or GG genotype.

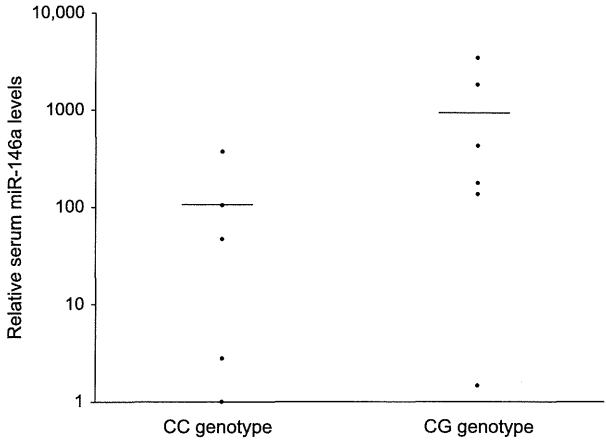

Figure 2 Serum concentrations of miR-146a in patients with dermatomyositis with CC genotype and those with CG genotype. miR-146a levels were measured with real-time polymerase chain reaction. Serum miR-146a concentrations are shown on the ordinate. The minimum value was set at 1. Bars show means

Table 1 Genotype frequencies of the miR-146 single nucleotide polymorphisms in patients with PM/DM and controls

Genotype	PM/DM ($n = 44$)	Control ($n = 107$)
CC	15 (34.1)[a]	51 (47.7)
CG	29 (65.9)	53 (49.5)
GG	0 (0)	3 (2.8)

DM, dermatomyositis; PM, polymyositis.
Comparisons of genotype distribution, using chi-square test, showed there was no significant difference between patients with PM/DM and controls ($P = 0.1295$).
[a]The numbers in parentheses indicate the percentage.

Table 2 Allele frequencies of miR-146 single nucleotide polymorphisms in patients with PM/DM and controls

Allele	PM/DM ($n = 44$)	Control ($n = 107$)
C	59 (67.0)[a]	155 (72.4)
G	29 (33.0)	59 (27.6)

DM, dermatomyositis; PM, polymyositis.
Comparisons of allele distribution, using chi-square test, showed there was no significant difference between patients with PM/DM and controls ($P = 0.3494$).
[a]The numbers in parentheses indicate the percentage.

Energy change by the single nucleotide polymorphism rs2910164

The expression levels of miR-146a are thought to be regulated by the stability between miR-146a (UGAGAACUGAAUUCCAUGGGUU) and its complementary strand (CCUC/GUGAAAUUCAGUUCUUCAG) in the miR-146a stem–loop precursor, at least partly. When the stability decreases, the expression level of the miRNA may be reduced. rs2910164 is located on the complementary strand. To determine whether the SNP rs2910164 can affect the stability, we calculated minimum free energy between miR-146a and its complementary strand using web-based bioinformatics: http://bibiserv.techfak.uni-bielefeld.de/rnahybrid/submission.html.[15] The minimum free energy of C allele is −24.0 kcal/mol, and

Table 3 Comparison of clinical and laboratory features among genotypes of miR-146a in patients with dermatomyositis

	Patients with CC genotype (n = 9)	Patients with CG or GG genotype (n = 16)	P value
Age (mean years)	58.7	54.6	0.655
Duration (mean months)	2.8	17.9	0.145
Clinical features			
Gottron	55.6	87.5	0.097
Heliotrope	44.4	56.3	0.440
Muscle weakness	100.0[a]	62.5	0.045
Lung involvement	66.7	30.8	0.110
Dysphagia	66.7[a]	9.1	0.009
Cancer	22.2	37.5	0.374
Joint pain	22.2	23.1	0.609
Laboratory findings			
ANA	77.8	57.1	0.290
IgG (mg/dl)	1359.1	1569.3	0.217
Creatine kinase (U/L)	797.6	2289.5	0.614
Myoglobin (ng/ml)	371.9	648.7	0.356
Aldolase (U/L)	9.3	21.2	0.391
%VC (%)	91.5	96.7	0.537
%DLco (%)	75.9	90.2	0.167
Chest radiograph change	44.4	25.0	0.319
ANA specificity			
Anti-Jo-1	33.3	12.5	0.230
Anti-SS-A	11.1	6.7	0.600
Anti-SS-B	11.1	6.7	0.600

ANA, antinuclear antibodies; Dlco, diffusion capacity for carbon mono-oxidase; IgG, immunoglobulin G; VC, vital capacity.
Unless indicated, values are percentages of patients.
[a]$P < 0.05$ vs. patients with CG+GG phenotype by Fisher's exact probability test.

Table 4 Comparison of clinical and laboratory features among genotypes of miR-146a in patients with clinically amyopathic dermatomyositis

	Patients with CC genotype (n = 4)	Patients with CG or GG genotype (n = 12)	P value
Age (mean years)	63.3	51.4	0.363
Duration (mean months)	7.7	2.6	0.091
Clinical features			
Gottron	50.0	75.0	0.365
Heliotrope	25.0	41.7	0.511
Muscle weakness	0.0	0.0	–
Lung involvement	25.0	41.7	0.511
Dysphagia	0.0	0.0	–
Cancer	0.0	16.7	0.550
Joint pain	0.0	33.3	0.272
Laboratory findings			
ANA	50.0	41.7	0.608
IgG (mg/dl)	1234.8	1331.4	0.361
Creatine kinase (U/L)	101.0	78.5	0.182
Myoglobin (ng/ml)	61.2	74.1	0.643
Aldolase (U/L)	5.4	5.5	0.537
%VC (%)	106.8	95.2	0.398
%Dlco (%)	92.9	78.9	0.309
Chest radiograph change	25.0	25.0	0.755
ANA specificity			
Anti-Jo-1	0.0	8.3	0.750
Anti-SS-A	0.0	8.3	0.750
Anti-SS-B	0.0	0.0	–

ANA, antinuclear antibodies; Dlco, diffusion capacity for carbon mono-oxidase; IgG, immunoglobulin G; VC, vital capacity.
Unless indicated, values are percentages of patients.

that of G allele was −26.8 kcal/mol. Thus, the MIRSNP rs2910164 may be functional, because the change G to C may decrease the stability between miR-146a and its complementary strand and decrease expression of the miRNA.

Finally, we compared serum miR-146a levels between five patients with DM with the CC genotype and six of those with the CG genotype. Consistent with the above prediction, the mean serum miR-146a was decreased in patients with the CC genotype, although not statistically significant (Fig. 2, P = 0.10).

Discussion

Recent studies indicate MIRSNPs may contribute to the clinical features of patients with various diseases. For example, MIRSNP in the miR-24 binding site on dehydrofolate reductase mRNA decreases the affinity of miR-24 and causes dehydrofolate reductase overexpression and resistance to methotrexate.[16] Investigation of MIRSNPs may be useful for evaluating therapeutic values as well as evaluating diagnosis or disease activity.

The clinical significance of rs2910164 has already been well investigated. For example, Akkz *et al.*[17] concluded that the miR-146a rs2910164 polymorphism has no

major role in genetic susceptibility to hepatocellular carcinogenesis. On the other hand, Shen *et al.*[18] suggested that breast/ovarian cancer patients with variant C allele tend to have an earlier age of cancer onset. Our study is the first to genotype rs2910164 in autoimmune diseases.

In this study, we presented two major findings. First, we could not find significant difference in the frequency of genotype distribution between controls and patients with PM/DM. On the other hand, the prevalence of weakness and dysphagia in patients with DM with CC genotype was significantly higher compared to patients with CG or GG genotype. Thus, miR-146a may be involved in the pathogenesis of muscle involvement. Because the number of patients included in this study is rather low for an SNP study, larger studies are needed in the future to confirm our result.

In addition, we suggest the possibility that rs2910164 may be functional and C allele may decrease the miR-146a expression, which may play a role in the pathogenesis of muscle involvement. Our result that the frequency of genotype distribution in patients with PM/DM is similar to that in controls may be compatible with the previous report that miR-146a expression levels did not increase or decrease in muscle tissue of patients with PM/DM, as described above.[3] As another limitation of this study, the calculation of minimum free energy between miR-146a and its complementary strand lacked statistical analysis. Functional assay should be needed to compare the stability of the miR-146a stem–loop precursor between the C and G allele. In addition, we could not find significant difference in serum miR-146a levels between patients with CC and CG, probably due to the small number of patients.

Taken together, our results suggest that investigating the genotype of patients with PM/DM, in particular DM, may be useful for predicting muscle involvement and understanding disease etiology. In addition, the most recent report indicates that a collagen-induced arthritis model mouse injected intravenously with miR-146a showed improvement of arthritis *in vivo*.[19] miRNA research in PM/DM may also lead to the development of novel therapeutic strategies.

References

1 Sontheimer RD. Cutaneous features of classic dermatomyositis and amyopathic dermatomyositis. *Curr Opin Rheumatol* 1999; 11: 475–482.

2 Friedman RC, Farh KK, Burge CB, Bartel DP. Most mammalian mRNAs are conserved targets of microRNAs. *Genome Res* 2009; 19: 92–105.

3 Eisenberg I, Eran A, Nishino I, *et al.* Distinctive patterns of microRNA expression in primary muscular disorders. *Proc Natl Acad Sci U S A* 2007; 104: 17016–17021.

4 Furer V, Greenberg JD, Attur M, *et al.* The role of microRNA in rheumatoid arthritis and other autoimmune diseases. *Clin Immunol* 2010; 136: 1–15.

5 Saunders MA, Liang H, Li WH. Human polymorphism at microRNAs and microRNA target sites. *Proc Natl Acad Sci U S A* 2007; 104: 3300–3305.

6 Bertino JR, Banerjee D, Mishra PJ. Pharmacogenomics of microRNA: a miRSNP towards individualized therapy. *Pharmacogenomics* 2007; 8: 1625–1627.

7 Mishra PJ, Banerjee D, Bertino JP. MiRSNPs or MiR-polymorphisms, new players in microRNA mediated regulation of the cell: introducing microRNA pharmacogenomics. *Cell Cycle* 2008; 7: 853–858.

8 Nakasa T, Miyaki S, Okubo A, *et al.* Expression of microRNA-146 in rheumatoid arthritis synovial tissue. *Arthritis Rheum* 2008; 58: 1284–1292.

9 Dai Y, Huang YS, Tang M, *et al.* Microarray analysis of microRNA expression in peripheral blood cells of systemic lupus erythematosus patients. *Lupus* 2007; 16: 939–946.

10 Sonkoly E, Stĺhle M, Pivarcsi A. MicroRNAs: novel regulators in skin inflammation. *Clin Exp Dermatol* 2008; 33: 312–315.

11 Bohan A, Peter JB. Polymyositis and dermatomyositis. *N Engl J Med* 1975; 292: 344–347.

12 Bohan A, Peter JB. Polymyositis and dermatomyositis. *N Engl J Med* 1975; 292: 403–407.

13 Gong J, Tong Y, Zhang HM, *et al.* Genome-wide identification of SNPs in microRNA genes and the SNP effects on microRNA target binding and biogenesis. *Hum Mutat* 2012; 33: 254–263.

14 Kroh EM, Parkin RK, Mitchell PS, Tewari M. Analysis of circulating microRNA biomarkers in plasma and serum using quantitative reverse transcription-PCR (qRT-PCR). *Methods* 2012; 50: 298–301.

15 Kanemaru H, Fukushima S, Yamashita J, *et al.* The circulating microRNA-221 level in patients with malignant melanoma as a new tumor marker. *J Dermatol Sci* 2011; 61: 187–193.

16 Mishra PJ, Humeniuk R, Longo-Sorbello GS, *et al.* A miR-24 microRNA binding-site polymorphism in dihydrofolate reductase gene leads to methotrexate resistance. *Proc Natl Acad Sci U S A* 2007; 104: 13513–13518.

17 Akkz H, Bayram S, Bekar A, *et al.* No association of pre-microRNA-146a rs2910164 polymorphism and risk of hepatocellular carcinoma development in Turkish population: a case-control study. *Gene* 2011; 486: 104–109.

18 Shen J, Ambrosone CB, DiCioccio RA, *et al.* A functional polymorphism in the miR-146a gene and age of familial breast/ovarian cancer diagnosis. *Carcinogenesis* 2008; 10: 1963–1966.

19 Nakasa T, Shibuya H, Nagata Y, *et al.* The inhibitory effect of microRNA-146a expression on bone destruction in collagen-induced arthritis. *Arthritis Rheum* 2011; 63: 1582–1590.